Tank Car Fire Failure Assessment using Combined Models

GCDOCS Workflow ID 65693178
TP 15493E
T44-3/24-2021E-PDF
978-0-660-40379-3

Submitted to Transport Canada

By

Jonathan McKinley, Jia Xue, Bruce W. Williams, and Su Xu

September 2021

DISCLAIMER

Natural Resources Canada makes no representations or warranties respecting the contents of this report, either expressed or implied, arising by law or otherwise, including but not limited to implied warranties or conditions of merchantability or fitness for a particular purpose.

Southern Rockies Consulting provided review of this document with no warranty, and with the understanding that Southern Rockies Consulting bears no responsibility for how it is used.

CanmetMATERIALS

GCDOCS Workflow ID 65693178

Finite Element Simulation of Rail Tank Car Creep Failure in an Engulfing Fire Scenario
By

Jonathan McKinley, Jia Xue, Bruce W. Williams, and Su Xu

Summary

An accident involving a rail tank car transporting flammable liquids such as crude oil, natural-gas condensates, or ethanol creates the potential for a pool fire. There have been a number of rail incidences in which flammable liquids have been involved. This presents a safety risk to the public and the environment. TDG would like to better understand the fire performance of rail tank cars to evaluate the applicable safety standards and regulations and to ensure that they provide a high level of safety

In order to investigate these concerns, TDG initiated research projects to investigate tank car failure at high temperature. From FY 2016/17 to 2018/19 CanmetMATERIALS (CMAT) conducted tensile and creep-rupture tests of TC 128B and ASTM 516 Grade 70, two of the most common steels used in manufacturing tank cars. During FY 2018/19 a constitutive material model that includes temperature-driven (25 °C to 800 °C) material softening and creep was implemented in finite element (FE) analysis software to enable detailed analysis of tank cars and tank car failures at high temperatures. CMAT then developed an FE model using specific tank car geometry to predict tank car failure under various pool fire conditions in 2018/19 and 2019/20.

CMAT had three main objectives for the 2020/21 fiscal year. These were to 1) Develop a simpler and faster engineering model for calculating material failure and validate it against the existing FE model. 2) Run a series of pool fire scenarios using temperature and pressure data from CanmetENERGY using both Models.3) Complete a comparison between AFFTAC, an established program for predicting tank car failure in pool fires, and CMAT's models.

CMAT developed an effective and time efficient engineering method for calculating the time to failure of a tank car in a pool fire scenario and validated it against their FE model. This model can be run in excel or other computational software. CMAT simulated 34 realistic pool fire scenarios in both their FE and engineering models. All cases survived at least 100 minutes. Only two cases resulted in failure within the 716 minutes run time. One failed due to a blocked PRV and one failed because it lacked thermal protection. These results demonstrate the importance of these key rail tank car safety systems.

Preliminary comparisons between CMAT's models and AFFTAC demonstrated some differences. Both AFFTAC and CMAT's models describe the high temperature behaviour of tank car

materials. They both can predict two failure modes; yield (plasticity) and creep. Both models are temperature dependent. As the temperature increases the yield stress decreases. At higher temperatures creep deformation occurs more rapidly at a given stress level than at lower temperatures. The realistic fire scenarios presented above did not provide sufficient data for comparing CMAT's models with AFFTAC. CMAT and AFFTAC produced different results in synthetic scenarios that were run for the purpose of comparison. Further investigation is recommended.

LIST OF ABBREVIATIONS

AXI	Axisymmetric
DOT	U.S. Department of Transportation
FEA	Finite Element Analysis
FE	Finite Element
RT	Room Temperature
UTS	Ultimate Tensile Strength
YS	Yield Strength
PRV	Pressure Relief Valve
SE	Single Element
TPS	Thermal Protection System

LIST OF SYMBOLS

ε	Strain
ε^{cr}	Creep Strain
ε_{11}^{cr}	Axial Creep Strain
ε_{22}^{cr}	Hoop Creep Strain
ε_{33}^{cr}	Thickness Creep Strain
$\dot{\varepsilon}^{cr}$	Creep Strain Rate
ε_{eq}	Equivalent Strain
E	Modulus of Elasticity
σ	Stress
σ_{axial}, σ_{11}	Axial Stress
σ_{hoop}, σ_{22}	Hoop Stress
σ_{33}	Through-thickness Stress
σ_u	Ultimate Tensile Stress
σ_y	Yield Stress
σ_{eq}	Equivalent stress (Von Mises stress)
p	pressure
Q	Activation Energy
R	Universal Gas Constant
r	Radius
T	Temperature
t	Thickness
τ	Time
γ	Parameter determining ellipse shape a^2/b^2

TABLE OF CONTENTS **PAGE**

1 INTRODUCTION

CanmetMATERIALS (CMAT) began working on a method to accurately predict creep and yield deformation in tank cars in 2015 with the eventual goal of being able to predict the time to failure of a tank car in an engulfing pool fire. CMAT began by characterizing common tank car steels TC128B and ASTM 516 Grade 70 (A516-70) at temperatures up to 800 °C. CMAT then developed creep and plasticity models to describe the materials' behaviour and implemented these material models into the finite element code Abaqus FEA. CMAT can use temperature and internal pressure boundary conditions as inputs supplied by CanmetENERGY though Transport Canada (TC) to run simulations of full-scale tank cars in fire scenarios and predict the time to rupture. In 2019 CMAT also began working on a simplified engineering model, which was developed as an alternative to CMAT's FEA model which is described in detail in the report Finite Element Simulation of Rail Tank Car Creep Failure in an Engulfing Fire Scenario (Jonathan Mckinley, 2020). The advantages of the engineering model are that it is faster, requires minimal computing power, and does not require specialized software to run. The model is presented in such a way that anyone with the necessary technical background can reproduce it. The preliminary engineering model developed in FY2019/20 compared well to the FEA model. The objective for FY2020/21 was to update the model to make it more generally applicable and conduct additional validation testing.

2 BACKGROUND

An accident involving a rail tank car transporting flammable liquids such as crude oil, natural-gas condensates, or ethanol creates the potential for a pool fire. The fire may subject a portion of the steel tank car to localized heating or, in the event of an engulfing fire, heating of the entire tank car. Due to the intense heating of the tank car steel, the tank car may fail, resulting in its contents being released and further fueling the fire. TDG is concerned about this because there have been a number of rail incidents in which flammable liquids have been involved, which presents a safety risk to the public and the environment. TDG would like to better understand the fire performance of rail tank cars to evaluate the applicable safety standards and regulations, and to ensure that they provide a high level of safety in the event of an incident because TDG has responsibility for rail safety standards.

In order to investigate these concerns, TDG initiated research projects to investigate tank car failure at high temperature, with an emphasis on crude oil transport. A series of project phases have already been conducted. In Fiscal Year (FY) 2016/17, at the request of TC, CMAT began investigating steel properties that influence the failure of tank cars in pool fire scenarios. The review found a lack of detailed and systematic studies of high-temperature mechanical response. CMAT determined that two key material behaviours contribute to the failure of a tank car at elevated temperatures. The first behaviour is material softening wherein the strength of the material decreases as the temperature increases. The second behaviour is creep which is permanent deformation that accumulates over time and can occur below a material's yield stress eventually resulting in rupture. Creep is more severe in materials that have been held at elevated temperatures such as those experienced during a crude oil pool fire.

From FY 2016/17 to 2018/19 CMAT conducted tensile and creep-rupture tests of TC 128B and ASTM 516 Grade 70, two of the most common steels used in manufacturing tank cars. During FY 2018/19 a constitutive material model that includes temperature-driven (25 °C to 800 °C) material

softening and creep was implemented in finite element analysis (FEA) software to enable detailed analysis of tank cars and tank car failures at high temperatures. CMAT then developed an FEA model using specific tank car geometry to predict tank car failure under various pool fire conditions in 2018/19 and 2019/20.

Also, in 2019/20 CMAT began work on a numerical engineering model that could be used to obtain similar results to the FEA model in a fraction of the time. The goal of this work is to develop engineering-level procedures for predicting tank car life in various fire scenarios. To that end, the tasks proposed in this document are aimed at a comparison between the FEA model, engineering model, and the industry-standard fire analysis software, "Analysis of Fire Effects on Tank Cars" (AFFTAC). AFFTAC performs dynamic, physics-based simulations of the heat exchange, stresses, expansion, and pressure relief events for a tank car exposed to fire. Models for each of these effects are combined to assess tank car performance in a specified fire condition. AFFTAC assumes thermal equilibrium between the vapour and liquid phases, which is justified under the assumption that venting occurs. Venting cools the vapour via the mechanical work of pushing lading through the PRV while liquid cools as it evaporates, placing its cooler molecules into the vapor phase. AFFTAC performs heat transfer calculations between the interior tank wall, the vapour touching it, and the liquid surface, the latter via radiation. It can model safety relief devices (valves or rupture disks), compute the flow of vapour, liquid, or mixture through those devices based on the calculated pressure differential, as well as the cooling associated with evaporation and ejection though the PRV. It also models the stress and strain of the tank and uses those results to predict the failure time of the tank. While it predicts creep AFFTAC is a fast and user-friendly numerical model that has wide acceptance and approval in the rail industry due to its simplicity and speed. In order to achieve this, AFFTAC uses assumptions and simplified equations to come to a result in seconds to minutes.

Results of AFFTAC modeling are used by regulatory agencies to evaluate and qualify thermal protection systems for tank cars, as per Section 8.2.7.1 of TP 14877. It is commonly used by industry to compare their designs and submit for approvals to the Association of American Railroads (AAR) who has the authority to approve tank car designs for submission to the US and Canadian Governments. Over the years of use, improvements have been made to AAFTAC's computational models in the areas of thermal protection, creep, and pressure relief devices, among others. However, AFFTAC's purpose has always been to provide a simple and accurate tool for the assessment of tank car designs, as opposed to providing a realistic simulation for research purposes. As such, there may be gaps between the results of AFFTAC and other models, and a greater understanding of the safety factor related to AFFTAC results is desired.

2.1 Tank Car Models

Models have been developed by various agencies for various purposes including investigating the fire performance of tank cars as well as heat transfer through a tank car into the lading. Some of these models served specific purposes (e.g., a steel material model), while others were for analysis of a complete tank car at high temperature conditions. The following list outlines a selection of these models, which are relevant to the current work:

1. Material model, developed by NRCan CMAT;
2. Tank Car 3D Computer-aided design (CAD) Model, developed by NRCan CMAT;

3. FEA model, developed by NRCan CMAT;
4. Engineering model, developed by NRCan CMAT;
5. Thermal and CFD models, developed by NRCan CanmetENERGY;
6. Process/Thermodynamic model, developed by NRCan CanmetENERGY;
7. AFFTAC, developed by RSI-AAR Tank Car Safety and Research Project, maintained by Scott Runnels at Southern Rockies Consulting;

Some such as AFFTAC have been in use for many years. Others have been developed more recently by NRCan, CMAT and CanmetENERGY.

Each of these models is described below. Specifically, their overall objective and relevance to the current work is described.

1. CMAT Material model

A material model is a mathematical description of how a material responds in various scenarios. CMAT's material models of TC128B and ASTM 516 Grade 70 describe plasticity and creep as a function of temperature, applied stress and time. CMAT's material model does not include heat transfer and therefore temperature is defined as a boundary condition.

Implementation: A general mathematical description that can be implemented in FEA code, a programming language, or even Microsoft Excel (MS Excel).

Inputs and outputs: The inputs are applied loads (stress) and temperature. The output is deformation (strain).

2. CMAT Tank Car 3D Computer-aided design (CAD) Model

The tank car CAD model is a geometrically-accurate three-dimensional (3D) description of a tank car structure. CMAT's CAD model is of a specific tank car geometry which represents a DOT 117 rail tank car from a specific manufacturer. As it is specific to the one tank car company, new CAD models would be required in order to represent different tank car geometries.

Inputs and outputs: Input is detailed geometric description. Result is a visual 3D representation of said geometry. Model does not have specific "output", however, the resulting 3D representation of a tank car be used as an input in a variety of FEA programs.

Implementation: Typically developed in specialized software such as SOLIDWORKS, 3D models can often be exported and imported into another software package. FEA software such as Abaqus often has its own 3D modelling functionality.

3. CMAT Finite Element Analysis (FEA) model

In this report, 'FEA models' and 'FEM' will refer specifically to 2D or 3D finite element models of solid deformation, and will be used in contrast to the 2D or 3D fluid dynamics models,

represented by the term 'CFD'. FEA models are models of how a structure responds to applied loads and boundary conditions. CMAT's tank car FEA model uses the material model for TC128B, the Tank Car 3D CAD model, and thermal and pressure boundary conditions to predict the creep and eventual failure of a tank car. Finite element models include sub-models such as the tank car 3D CAD model as an input.

Inputs and outputs: The input for this model is a tank car 3D CAD model, mesh (the discretization of the Tank Car 3D CAD model into small sections for computational purposes), material model (description of material behaviours) and boundary conditions (loads such as body weight or external forces and temperature or heat transfer rate). The list of outputs can be broad and varied, but typically include full field contours of stress and strain, but may also include accelerations, total deformation, and external forces. The outputs may be static or vary as a function of time. For creep rupture simulations, the accumulated creep strain is used as the indication of failure (rupture) which is determined by the state of stress (e.g.: von Mises stress or three principle stresses).

Implementation: Finite element models run in specialized software. Typically, it is impossible or very difficult to export the entire model and transfer to another FEA program.

4. CMAT Engineering model

CMAT's current engineering model uses the same material model and geometry as the FEA model, though with a simplified implementation. Additional assumptions and simplifications, such as simplified geometry and assumption of linear stress-strain response, result in a simulation that can be run in a fraction of the time.

Inputs and outputs: Similar to FEA, the material model, tank geometry and boundary conditions can be considered inputs. Time to rupture is the output.

Implementation: Spreadsheet such as Excel or programming language such as Python or Fortran/MATLAB.

5. CanmetENERGY Thermal and CFD models

When conducting a thermal model of a tank car in a pool fire it is important to consider both the heat transfer from the fire by radiation and convection to the surface of the tank car and the heat transfer by conduction through the wall and by convection of the lading within the tank car. CanmetENERGY has conducted simulations of a tank car exposed to fire using computational fluid dynamics (CFD).

Inputs and outputs: Inputs are external thermal boundary conditions, thermal and fluid properties of tank car components and contents. Output is full 2D temperature map of tank car over time and internal pressure.

Implementation: The CanmetENERGY CFD simulation is conducted in ANSYS. Some codes can run FEA and CFD or allow CFD and FEA to be run simultaneously. Like FEA models, CFD models cannot be easily transferred to another program.

This model is not being updated under this SOW in FY2020/21, however, work is being performed by CanmetENERGY under a separate SOW and inputs were received for Task 2.1.

6. CanmetENERGY Process/Thermodynamics model

CanmetENERGY has conducted simulations using the process simulation software HYSYS to predict the pressure, temperature, and the chemical reactions that occur in a tank car.

Inputs and outputs: External temperature boundary conditions, properties of lading. Output is 2D bulk fluid temperature over time and tank pressure.

Implementation: HYSYS.

This model is not being updated under this SOW in FY2020/21, however, CanmetENERGY is performing additional work under a separate SOW and inputs were received for Task 2.1 this FY.

7. AAR-RSI AFFTAC

AFFTAC (Analysis of Fire Effects on Tank Cars) is specialized software for modeling the thermal and structural response of a tank car in a fire. AFFTAC was built to be simple to use and quick to run and therefore assumes 2D geometry for many calculations, however, when performing volumetric and surface area calculations the length and end caps are included. AFFTAC computes the heat exchange between a tank car in both pool fire and torch fire scenarios.

Inputs and outputs: Inputs include fire and lading temperatures, tank geometry and construction details, orientation information, lading data, PRV models, tank material strength information, and a variety of thermal protection system (TPS) setups, which can include defects, while the outputs are temperature and pressure histories with time as well as time to rupture.

Implementation: Custom single-purpose software.

3 ENGINEERING MODEL

The engineering model predicts the strain at the point of peak temperature due to creep over time based on both stress and temperature. The model then checks for failure due to material yielding and accumulated creep strain. This model was developed using insight gained from CMAT's full scale Finite Element (FE) simulations. The following assumptions were made to simplify calculations:

1) The point of peak deformation and therefore failure occurs at the point of peak temperature.
2) Failure occurs due to localized accumulated strain.

These assumptions are based on the FE simulations that have been run to date.

The engineering model is primarily a material model which predicts the strain that results from an applied stress. The stress state of the tank car shell is relatively simple to calculate. The material's behaviour, such as yield stress and creep rate are strongly dependent on temperature which is constantly changing in a fire scenario. The model must also account for the effect of accumulated strain. The objective of this report is to describe the model's calculations so that they may be reproduced.

The accuracy of any prediction is dependent on the accuracy of the input data. The required inputs are the pressure inside the tank car, the peak wall temperature as a function of time, and the geometry of the tank car, specifically the wall thickness and the outer shell dimensions. An example of the temperature and pressure boundary conditions required are shown in Figure 1: Peak temperature and pressure versus time for a tank car in a fire scenario (example data)

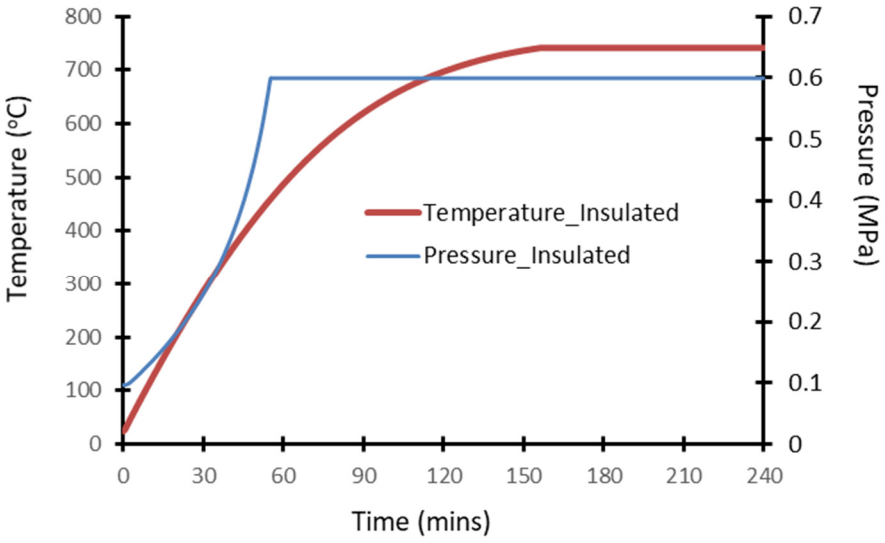

Figure 1: Peak temperature and pressure versus time for a tank car in a fire scenario (example data)

3.1 Tank Car Geometry

Transport Canada provided CanmetMATERIALS with detailed drawings of a 30,500 Gallon DOT-117 rail tank car which was used to develop a FE model in Abaqus as shown in Figure 2. Both ends of the tank car are inclined at 1.04° from horizontal. Each part of the support structure that directly contacts the tank car shell was included in the analysis, as were any features that could add reinforcement or weaken the tank structure, such as the manway. Welds were not modelled due to previous work conducted which indicated that the welds are not critical in high temperature failure. ((*Finite Element Simulation of Rail Tank Car Creep Failure in an Engulfing Fire Scenario*, Jonathan McKinley, 2020).). The rest of the support structure was simplified to a structure that would provide a similar level of stiffness with less complexity. The engineering model uses simplified geometry of a cylindrical shell with ellipsoidal heads.

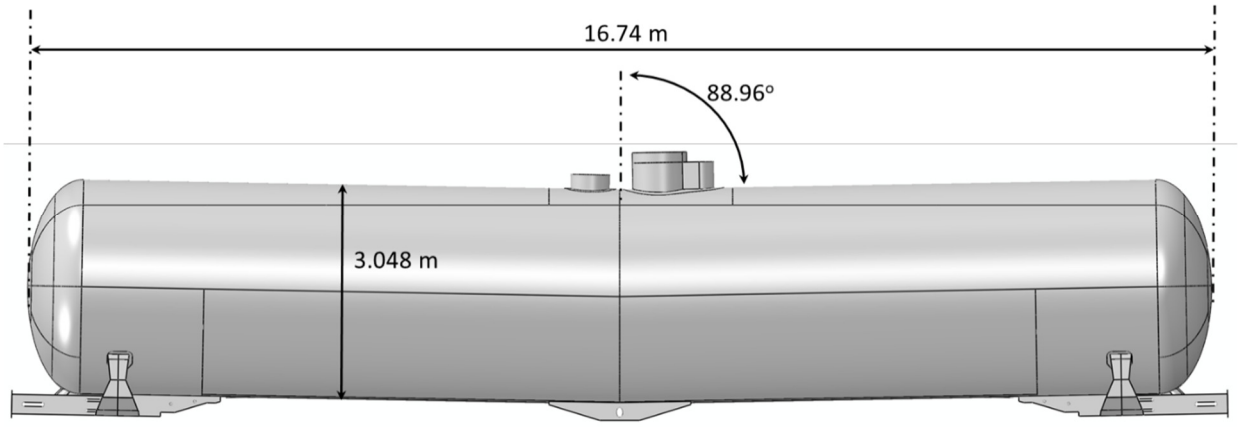

Figure 2: Dimensions of the tank car

3.2 Notation

The following conventions are used in this document.

Superscript

Superscript is used to provide information about or describe a value; for example:

ε^p, σ^p	Denote plastic strain and plastic stress
$\varepsilon^{cr}, \sigma^{cr}$	Denote creep strain and creep stress

Direction and Coordinate System

Directions of stress and strain will be denoted by two subscript numbers following the symbol such as ε_{11}.

Stresses, strain, and forces occur in three directions on a tank car shell. The axial direction is aligned along the length of the tank car and denoted by 11. An axial stress, σ_{11} , stretches or compresses the tank car along its length. The hoop or circumferential direction is denoted by 22. A hoop strain, ε_{22}, would increase or decrease the diameter of the tank. The third direction is through the thickness of the tank shell, ε_{33}, which would increase or decrease the thickness of the tank shell.

Increment

A second subscript is used to identify the time increment; n is the current increment, n-1 is the previous increment. Therefore, ε_{11_n} is the axial strain in the current increment, and $\varepsilon_{11_{n-1}}$ is the axial strain in the previous increment. Initial conditions are represented with a subscript 0, such that ε_{11_0} is the initial axial strain. Only equations that require values from other increments include these subscripts. An equation without an increment subscript should be assumed to use values entirely from the current time increment.

Other Subscripts

σ_u denotes the ultimate tensile stress, σ_y the yield stress, and σ_{eq} the equivalent stress (Von Mises stress). All are scalar values that quantify the three-dimensional state of stress at a material point.

3.3 Engineering Model Procedure

The engineering model was developed as a procedure which can be implemented as desired by the user. This was done primarily so that it can easily be updated or modified in the future, such as to add a new material. The calculations can be completed in a spreadsheet (ex. MS Excel) or a simple program written in Fortran or scientific Python. CMAT's own MS Excel spreadsheets will be shared with Transport Canada. A flowchart of the model is shown in Figure 3. The major steps of the process are also numbered in the flowchart and CMAT's spreadsheet.

The engineering model operates in the time domain, as does the FE model. The input state variables change with time. Creep strain and plastic strain accumulate. They do not return to zero if the pressure in the tank car or the temperature are reduced. The calculations are therefore performed using time steps or increments similar to the forward difference method. In each time increment the strain state and geometry (shell thickness) is read from the previous increment and then the temperature, pressure and material properties are updated. The stress is then calculated based on the pressure and tank car geometry, and the strain and the shell thickness reduction can be recalculated. The model also checks for plasticity (yielding) or tensile failure at each time increment. Calculations terminate if the UTS is exceeded.

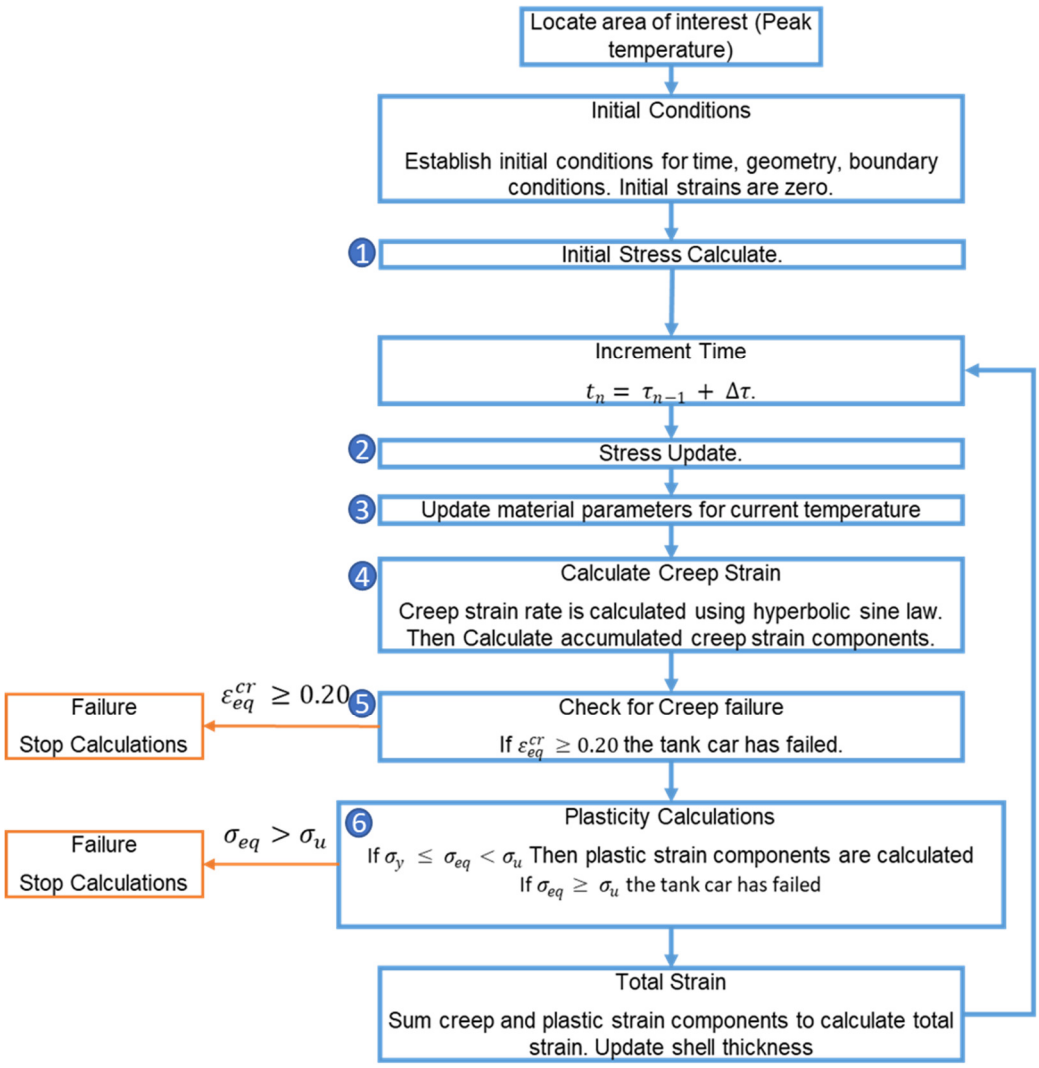

Figure 3: Flow chart of the engineering model

Establish Location of Interest

The model must first identify the location of interest, which is the point most likely to result in failure, and the location that will see the most creep deformation. Previous FE simulations have shown that this is the point of highest temperature. This occurs because the material's properties are dependent on temperature. The highest temperature point will always have the highest rate of creep and the lowest yield strength. The location of the peak temperature will be determined from the temperature and pressure inputs. It is possible that a scenario could arise with multiple points of interest due to the location of the peak temperature changing, but this has not been observed to date. If it does occur then this procedure should be repeated for each location of interest to determine the point at which failure will occur in the smallest timestep. Figure 4 shows an example of the temperature distribution, based on the 2D input from CanmetENERGY, of an upright and full tank car.

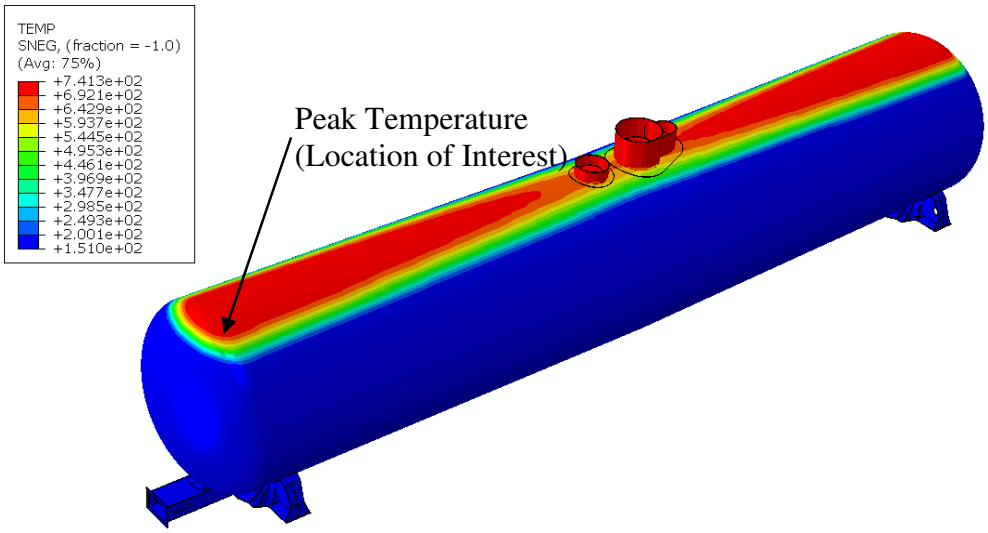

Figure 4: An example of temperature distribution applied to a full scale tank car for FE simulations.

Initial Conditions

Initial conditions are the starting values for parameters that will be used in future calculations.

The initial conditions that are required are summarized below.

t_0	Initial wall thickness of tank
p_0	Initial pressure inside tank car
$\varepsilon^t_{xx_0} = \varepsilon^{cr}_{xx_0} + \varepsilon^p_{xx_0} = 0$	All initial strain components and resulting equivalent strains are set to zero at the beginning of calculations
$\tau_0 = 0$	Initial time is zero

Calculate Initial Stress (① in Figure 3)

Two methods are available to calculate the initial stress conditions as shown in Figure 5. If the peak stress occurs in the main cylindrical tank shell, simple thin-walled pressure vessel calculations can be used. If the peak stress occurs in the elliptical head, then the provided equations can be used (1), (2).

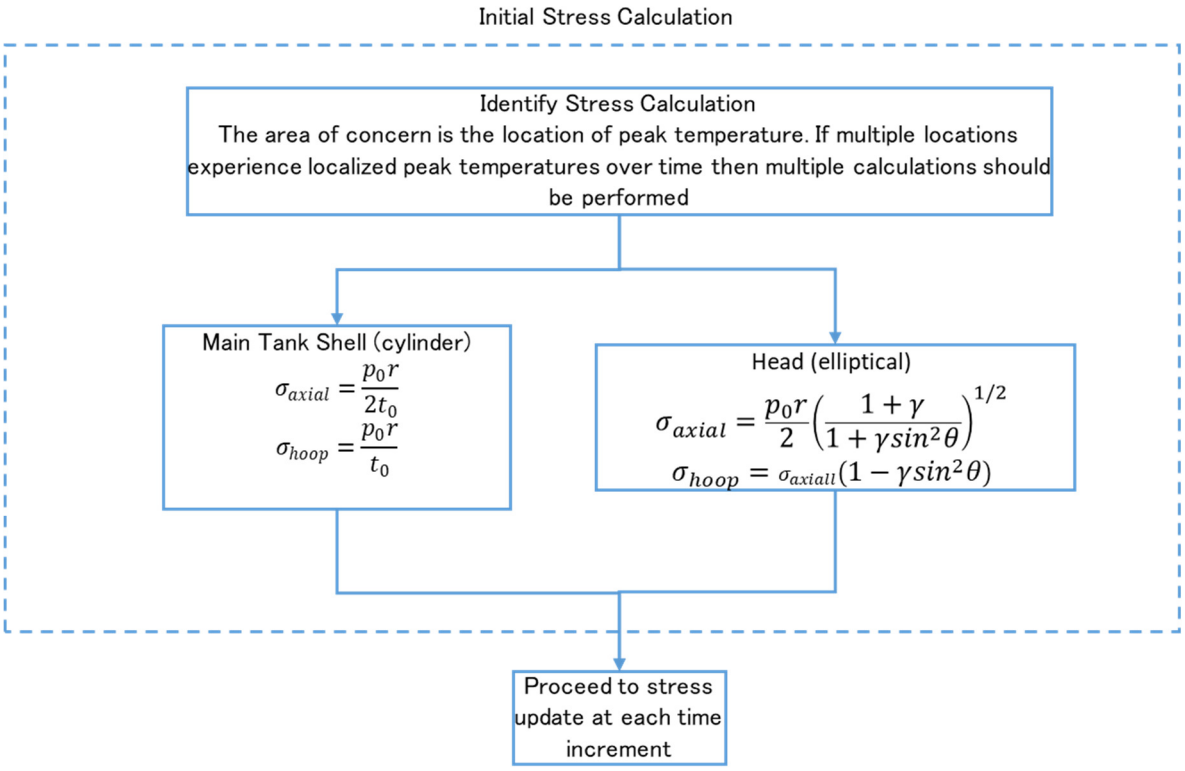

Figure 5: Illustration of the initial stress calculation procedure

Main tank shell stress equations:

$$\sigma_{11_0} = \sigma_{axial} = \frac{p_0 r}{2t_0} \tag{1}$$

$$\sigma_{22_0} = \sigma_{hoop} = \frac{p_0 r}{t_0} \tag{2}$$

where p is pressure, r is radius, and t is thickness. The tank car is assumed to behave as a thin walled pressure vessel therefore $\sigma_{33_0} = 0$. This is a standard assumption for this type of analysis. Previous FEA simulations did allow for variations in through thickness stress, strain, and temperature. The influence was not significant and the thin walled assumption was shown to be valid.

The peak temperature has always occurred at the highest point on the tank car in all of the boundary condition data that CMAT has received. This is due to the presence of a vapour space which has a reduced capacity to remove heat than the lading. When the tank car is tilted the peak temperature occurs in the tank head. The stress state in the tank head is much more complex than in the main shell as shown in the FEA results in Figure 6. In this orientation, the hoop stress transitions from compression to tension.

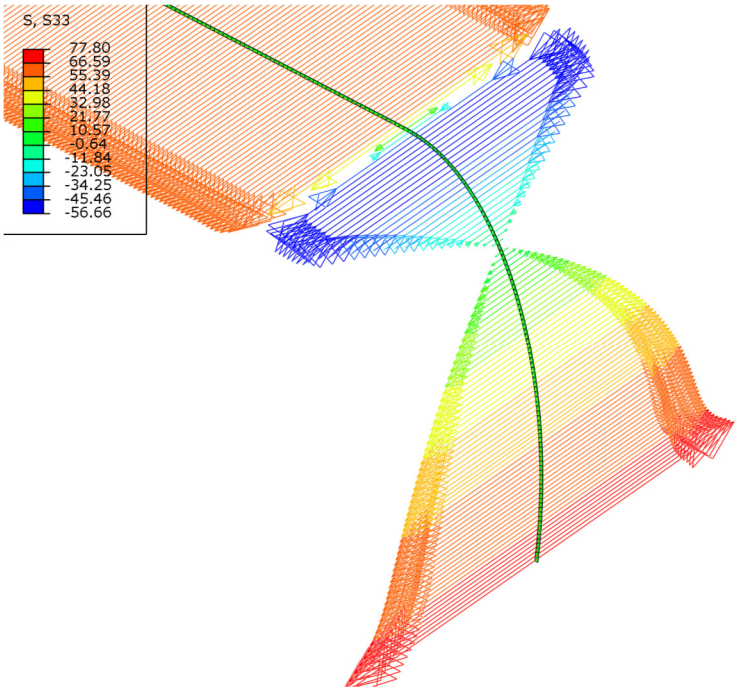

Figure 6: Hoop stress distribution at the tank head predicted by FEA

The formulas published by P. Baličević for stress in the elliptical head (Baličević P, 2008) were used to capture the stress distribution, which agree well with the FEA prediction as shown in Figure 7. A major ellipsoid semi-axis is equal to the cylindrical parts radius (a = R), and a minor semi-axis is equal to the head height (b = H). $\gamma = \frac{a^2}{b^2} - 1$ is a parameter that describes the form of the ellipse, where a is the maximum radius and b is the minimum radius. Figure 8 shows the dimension of a cylindrical vessel with an ellipsoid of revolution shaped head as used in Baličević's calculations. While this functionality is possible, it was not used for this year's work as no temperature and pressure input data was available for the elliptical heads.

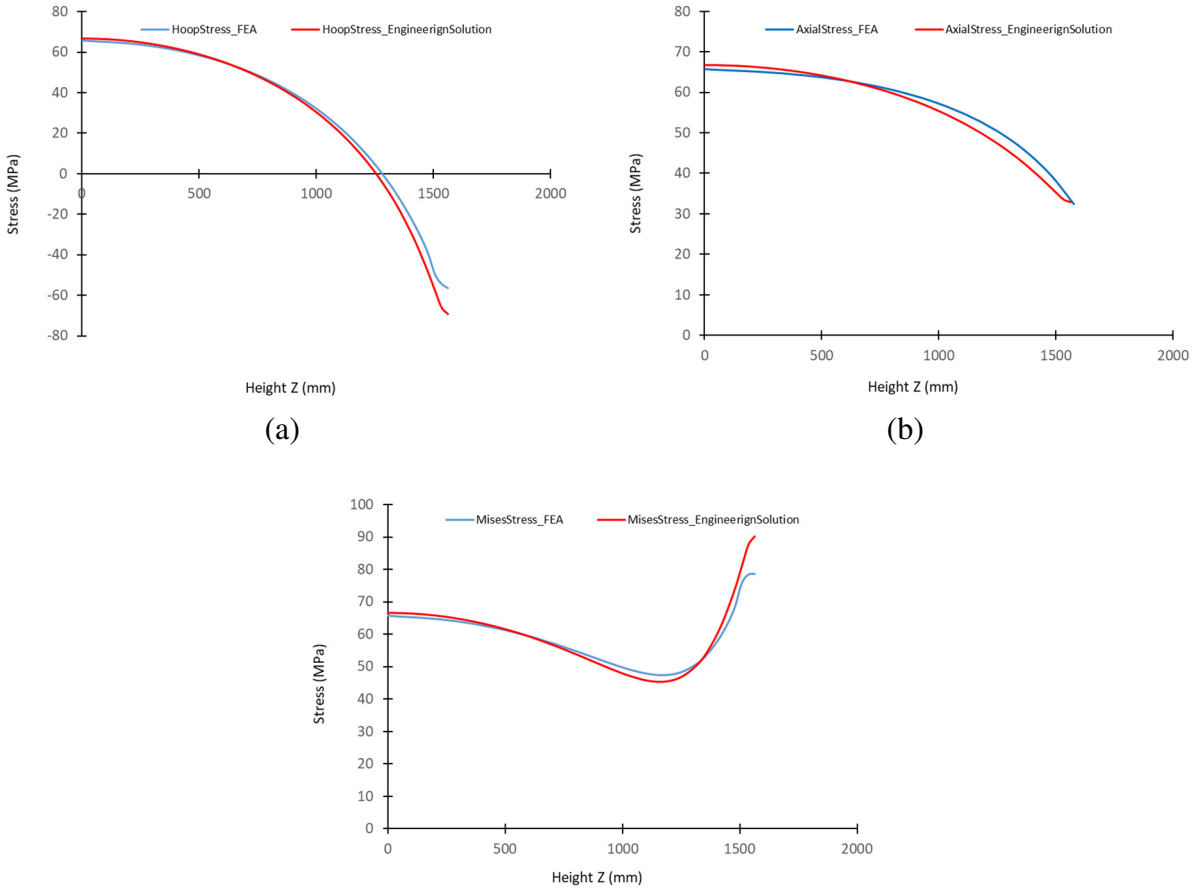

Figure 7: Comparison of FEA and analytical stress calculation of a) hoop stress, b) axial stress, and c) the resulting Von Mises stress at tank car head

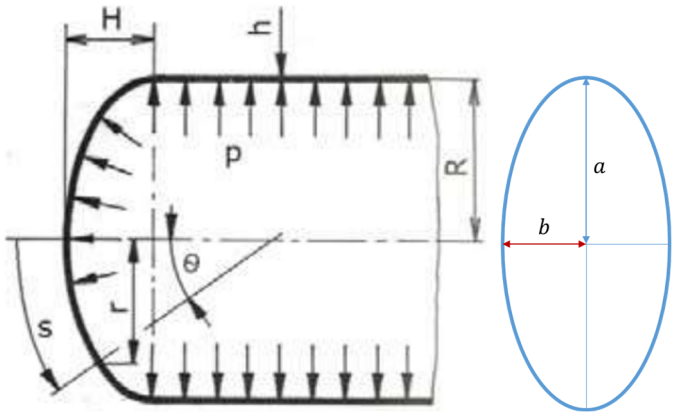

Figure 8: Pressure vessel with ellipsoidal head and ellipse dimensions [1]

Baličević's calculations of axial and hoop stress in the elliptical tank head are given below:

$$\sigma_{11_0} = \sigma_{axial} = \frac{pr}{2}\left(\frac{1+\gamma}{1+\gamma sin^2\theta}\right)^{1/2} \quad (3)$$

$$\sigma_{22_0} = \sigma_{hoop} = (1-\gamma sin^2\theta)\sigma_{axial} \quad (4)$$

Once the initial stress components $\sigma_{11_0}$and $\sigma_{22_0}$are calculated the initial Von Mises or equivalent stress σ_{eq_0}can be calculated using the principle stress formulation on the Von Mises equation (5). The shear stress components are found to be insignificant and thus not included in the calculation of Von Mises stress for simplicity.

$$\sigma_{eq} = \sqrt{\frac{(\sigma_{11}-\sigma_{22})^2 + (\sigma_{22}-\sigma_{33})^2 + (\sigma_{33}-\sigma_{11})^2}{2}} \quad (5)$$

For the main shell where $\sigma_{22} = 2\sigma_{11}$the equation is simplified to

$$\sigma_{eq} = \sqrt{3}\cdot\sigma_{11} \quad (6)$$

Increment Time

This is the first repeating step of the procedure at increment $n+1$ (or at increment 1 if this is the first time completing the step). The time is set to $\tau_n = \tau_{n-1} + \Delta\tau$ where the previous time is τ_{n-1} and $\Delta\tau$ is the length of the increment. CMAT typically uses the same increment as the provided temperature and pressure inputs for simplicity. In this work, the temperature and pressure boundary conditions were provided with a 4 minute increment therefore for simplicity an increment of 4 minutes was used for the FEA modelling and engineering calculations. A time increment that is too large can result in inaccuracy. If reducing the time increment results in a change in the final answer of greater than 1% then the initial time increment was too large. At least 100 increments are recommended as a starting point. More increments might be necessary if the temperature or pressure increase rapidly.

Next the pressure p_n and temperature T_n of the current time step are read from the supplied boundary conditions. Interpolation may be used if the engineering model time increments do not match the time increments of the supplied temperature and pressure data.

Stress Update (② in Figure 3)

The stress is updated using the strain from the previous step and the current pressure. The change of stress in the wall of the tank car is dependent on the internal pressure and the geometry of the tank. As the wall thins the stress increases. Since the relationship is linear the initial calculations do not need to be repeated. The stress can be updated using the equations below, which update equations (1) and (2) to account for changing pressure and shell thickness:

$$\sigma_{22_n} = \sigma_{22_0} \cdot \frac{P_n}{P_0} \cdot \frac{1}{1 - \varepsilon^t_{33_{n-1}}}$$
$$\sigma_{11_n} = \sigma_{11_0} \cdot \frac{P_n}{P_0} \cdot \frac{1}{1 - \varepsilon^t_{33_{n-1}}} \quad (7)$$

The equivalent stress at increment n can then be calculated using equation (5) or (6).

Update Material Parameters (③ in Figure 3)

The material's creep and yield behaviour are dependent on temperature. The parameters that will be used in creep and plasticity calculations can now be updated for the specific conditions of this increment. The equation for creep strain rate as a function of stress and temperature is shown below (10). The constants *A, B,* and *n'* are a function of temperature. The constants for TC128B and A516-70 are shown in and Table 1 and

Table 2 below (Jonathan Mckinley, 2020).

$$\dot{\varepsilon}^{cr}_{eq} = A\left(\sinh B\sigma_{eq}\right)^n exp\left(-\frac{Q}{RT}\right) \quad (8)$$

Table 1: Constants for hyperbolic sine model of TC128B steel

Temperature	***A***	***B***	***n'***	***Q***
°C	**min^{-1}**	**MPa^{-1}**	**---**	**J mol^{-1}**
800	1.03E+06	0.01452	4.131	168283
700	7.36E+06	0.01255	4.822	168283
600	4.00E+07	0.00607	5.2	168283
550	73966740.3	0.00429	5.50046	168283
400	0	0.00429	5.50046	168283

Table 2: Constants for hyperbolic sine model of A516-70 steel

Temperature °C	***A*** **min^{-1}**	***B*** **MPa^{-1}**	***n'*** ---	***Q*** **J mol^{-1}**
400	0	0.00391	7.406	168283
500	1.06E+08	0.00391	7.406	168283
600	44941600	0.00664	5.206	168283
700	7356130	0.01314	4.639	168283
800	949740	0.01594	4.591	168283

The temperature-dependent coefficients for this increment's temperature are calculated using linear interpolation (9).

$$y_n = y_a + \frac{T_n - T_a}{T_b - T_1} \cdot (y_b - y_a) \tag{9}$$

Where T_n is the temperature of the current time increment, T_a is the temperature below T_n from Table 1 or

Table 2 and $T_b$is the temperature above. y is the parameter of interest.

Note that the lowest temperature experiments conducted by CMAT that had any measurable creep were at 550 °C for TC128B and 500 °C for A516. No creep will occur at 400 °C or below.

The hyperbolic sine creep model, as used in the FEA and engineering models, was updated with new coefficients based on this data.

The ultimate tensile strength (UTS, σ_u) is a function of temperature and updated at each increment. Equations to calculate UTS as a function of temperature are shown below.

TC128B:
$$\sigma_u(T) = \begin{cases} 662 - 0.2668\,T & RT \leq T \leq 400^o\,C \\ 1161.667 - 1.50667\,T & 400^oC < T \leq 700^oC \\ 201 - 0.12\,T & 700^oC < T \end{cases} \tag{10}$$

A516-70:
$$\sigma_u(T) = \begin{cases} 629.667 - 0.26667\,T & RT \leq T \leq 400^oC \\ 1085.0 - 1.4050\,T & 400^oC < T \leq 700^oC \\ 182.0 - 0.115\,T & 700^oC < T \end{cases} \tag{11}$$

Similarly the yield stress can be calculated using the equation below (12). The constants for TC128B and A516-70 are provided in
Table 3. The UTS and yield strength are shown graphically in Figure 9. Details regarding the material properties can be found in the previous report (*Finite Element Simulation of Rail Tank Car Creep Failure in an Engulfing Fire Scenario,* Jonathan McKinley, 2020).

$$\sigma_y(T) = \sigma_{y0} exp\left(-\frac{1}{2}\left[\frac{T-RT}{r_3}\right]^{r_1} - \frac{1}{2}\left[\frac{T-RT}{r_4}\right]^{r_2}\right) \tag{12}$$

Table 3: Constants for temperature-dependent yield strength of TC128B and A516-70

	TC128B	**A516-70**
$\boldsymbol{\sigma_{y0}}$ [MPa]	354	396
$\boldsymbol{r_1}$	3.875	5.5
$\boldsymbol{r_2}$	0.795	1
$\boldsymbol{r_3}$ [°C]	612.763	610
$\boldsymbol{r_4}$ [°C]	529.184	550

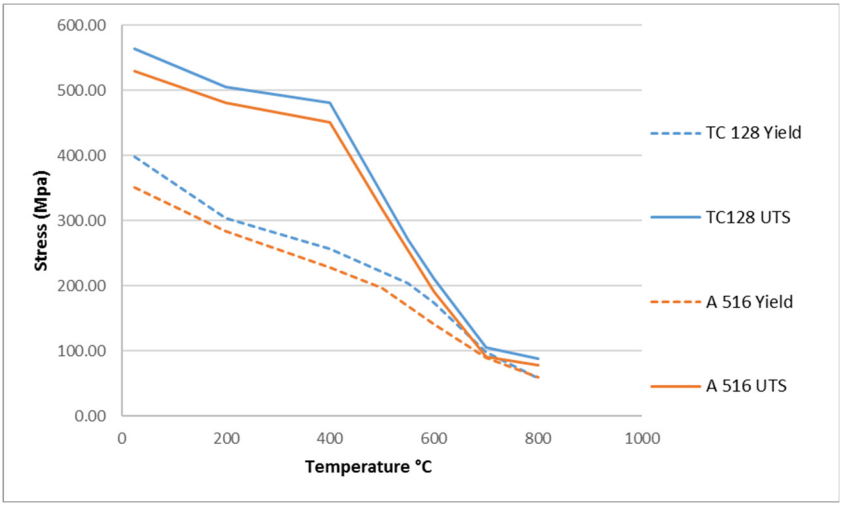

Figure 9: Yield stress and UTS of A516-70 and TC128B as a function of temperature

Calculate Creep Strain (④ in Figure 3)

Now that the temperature-specific material parameters are known the additional creep strain of this increment can be calculated. The equivalent creep strain rate, $\dot{\varepsilon}_{eq}^{cr}$, for this increment is calculated using equation (8), and the parameters from the previous step.

$$\dot{\varepsilon}_{eq}^{cr} = A\left(\sinh B\sigma_{eq}\right)^{n} exp\left(-\frac{Q}{RT}\right) \tag{8}$$

The components of the creep strain rate can then be calculated using the equations:

$$\begin{aligned}
\dot{\varepsilon}_{11}^{cr} &= \frac{\dot{\varepsilon}_{eq}^{cr}}{\sigma_{eq}}\left[\sigma_{11} - \frac{1}{2}\cdot(\sigma_{22}+\sigma_{33})\right] \\
\dot{\varepsilon}_{22}^{cr} &= \frac{\dot{\varepsilon}_{eq}^{cr}}{\sigma_{eq}}\left[\sigma_{22} - \frac{1}{2}\cdot(\sigma_{11}+\sigma_{33})\right] \\
\dot{\varepsilon}_{33}^{cr} &= \frac{\dot{\varepsilon}_{eq}^{cr}}{\sigma_{eq}}\left[\sigma_{33} - \frac{1}{2}\cdot(\sigma_{11}+\sigma_{22})\right]
\end{aligned} \tag{13}$$

These equations are based on plasticity theory with the following additional assumptions; the material remains isotropic, there is no change in volume, and the strain components are proportional to the applied stress components. A complete formulation including shear strains can be found in *Plasticity for Structural Engineers* (W.F. Chen, 1988).

The accumulated equivalent creep strain is then updated by multiplying the creep strain rate by the time increment length and adding it to the creep strain from the previous increment:

$$\begin{aligned}
{\varepsilon_{11}^{cr}}_{n} &= {\dot{\varepsilon}_{11}^{cr}}\cdot\Delta\tau + {\varepsilon_{11}^{cr}}_{n-1} \\
{\varepsilon_{22}^{cr}}_{n} &= {\dot{\varepsilon}_{22}^{cr}}\cdot\Delta\tau + {\varepsilon_{22}^{cr}}_{n-1} \\
{\varepsilon_{33}^{cr}}_{n} &= {\dot{\varepsilon}_{33}^{cr}}\cdot\Delta\tau + {\varepsilon_{33}^{cr}}_{n-1} \\
{\varepsilon_{eq}^{cr}}_{n} &= {\dot{\varepsilon}_{eq}^{cr}}\cdot\Delta\tau + {\varepsilon_{eq}^{cr}}_{n-1}
\end{aligned} \tag{14}$$

Check for Creep Failure (⑤ in Figure 3)

Previous work has shown that strain at failure is dependent on temperature. In practice, the strain rate accelerates exponentially as the material approaches failure, and therefore changes to the strain-failure criterion have little effect on the time to failure. 20% strain will continue to be used as the failure strain. If $\varepsilon_{eq}^{cr} \geq 0.20$ then the tank car is considered to have failed. If not the algorithm continues to the next step.

More details on creep failure can be found in CMAT's previous reports (Jonathan Mckinley, 2020).

Plasticity Calculations (⑥ in Figure 3)

In this step we calculate whether the tank car has failed outright due to the stress surpassing the UTS and whether any plasticity has occurred.

If $\sigma_{eq} < \sigma_y$ then no plasticity has occurred and ε_{eq}^{pl}=0. No calculations are required. Proceed to the next step.
If $\sigma_y \leq \sigma_{eq} < \sigma_u$ then plastic deformation has occurred, and ε_{eq}^{p} must be calculated.
If $\sigma_{eq} \geq \sigma_u$ for the increment then the tank car has failed.

In almost all simulations conducted by CMAT the amount of plasticity is small compared to the creep strain therefore these calculations focus on calculating creep deformation. If $\sigma_{eq} \geq \sigma_y$ the engineering calculations can continue however it is recommended that finite element simulations be conducted to verify the results if the plastic strain is large.

The equivalent plastic strain is calculated using this equation

$$\varepsilon_{eq}^{p} = \ln\left(1 - \frac{\sigma_{eq} - \sigma_y}{\sigma_u - \sigma_y}\right)\left(\frac{1}{-m}\right) \tag{15}$$

Where $m = 17$ (as determined in *Finite Element Simulation of Rail Tank Car Creep Failure in an Engulfing Fire Scenario*, Jonathan McKinley, 2020.) across all temperatures

This is a rearrangement of the Voce equation

$$\sigma_{eq} = \sigma_y + \left(\sigma_u - \sigma_y\right)\left[1 - \exp\left(-m \cdot \varepsilon_{eq}^{p}\right)\right] \tag{16}$$

The individual plastic strain components can then be calculated

$$\varepsilon_{11}^{p} = \frac{\varepsilon_{eq}^{p}}{\sigma_{eq}}\left[\sigma_{11} - \frac{1}{2} \cdot (\sigma_{22} + \sigma_{33})\right]$$
$$\varepsilon_{22}^{p} = \frac{\varepsilon_{eq}^{p}}{\sigma_{eq}}\left[\sigma_{22} - \frac{1}{2} \cdot (\sigma_{11} + \sigma_{33})\right] \tag{17}$$

$$\varepsilon_{33}^{p} = \frac{\varepsilon_{eq}^{p}}{\sigma_{eq}}\left[\sigma_{33} - \frac{1}{2}\cdot(\sigma_{11}+\sigma_{22})\right]$$

Total Strain

The total strain ε^{t}components can then be calculated

$$\begin{aligned} \varepsilon_{eq}^{t} &= \varepsilon_{eq}^{p} + \varepsilon_{eq}^{cr} \\ \varepsilon_{11}^{t} &= \varepsilon_{11}^{p} + \varepsilon_{11}^{cr} \\ \varepsilon_{22}^{t} &= \varepsilon_{22}^{p} + \varepsilon_{22}^{cr} \\ \varepsilon_{33}^{t} &= \varepsilon_{33}^{p} + \varepsilon_{33}^{cr} \end{aligned} \tag{18}$$

The shell thickness can then be calculated:

$$\begin{aligned} t_n &= t_0 \cdot (1+\varepsilon_{33}^{t}) \\ t_0 &= initial\ shell\ thickness \end{aligned} \tag{19}$$

ε_{33}^{t} will be used in the next increment's stress value. The other components of strain are not used but they are useful for comparison with FEA calculations.

Return to Increment Time

If the tank car has not failed it returns the *Increment Time* step and calculations continue.

The engineering model is developed based on the stress state in either the wall or head of the tank car. If predictions are required for more complex stress states, such as in a localized hot zone, then it is suggested to use the FEA model to capture the complex interaction between creep and plastic strain.

4 ENGINEERING MODEL VALIDATION

The engineering model was validated by comparison to the finite element model described in the report *Finite Element Simulation of Rail Tank Car Creep Failure in an Engulfing Fire Scenario* (Jonathan Mckinley, 2020). The engineering model was also compared to the FEA cases presented in this report which are described in later sections. Some discussion is included here for validation purposes. Example data from these comparisons are shown in Figure 10 and Figure 11. In all cases the predicted strain and stress were very similar. The accuracy of the Case 33 results was improved by reducing the time increment to 0.1 minute. This was the only case with this issue. Linear interpolation was used to determine the temperature and pressure at the additional time steps. It

was also the only case with significant amount of plasticity. It is recommended that any case that exhibits plasticity should be run with a reduced time step or in FEA.

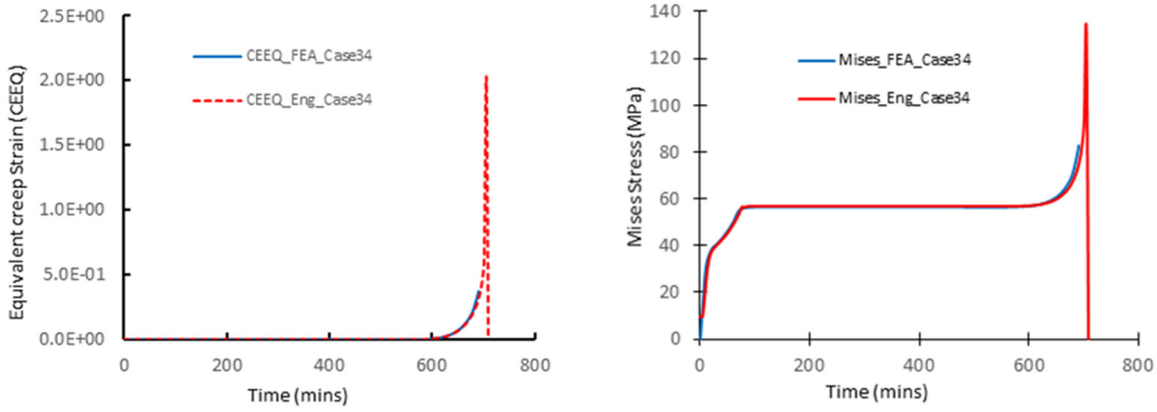

(a) (b)

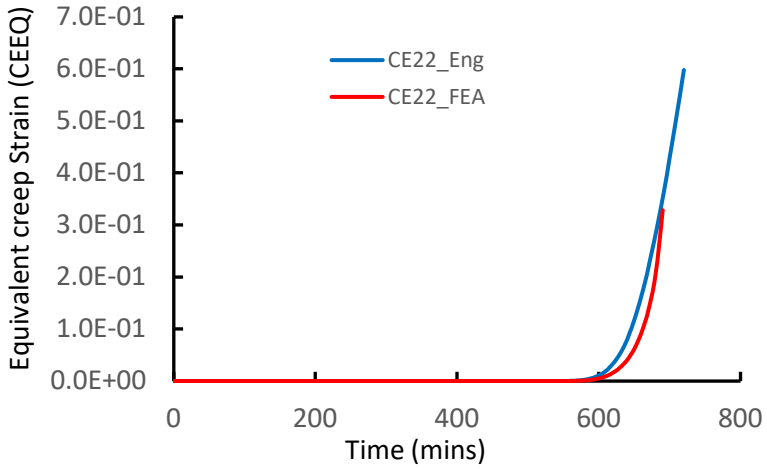

(c)

Figure 10: Comparison of engineering model and FEA results for Case 34: bare shell. (a) CEEQ is equivalent plastic strain ε_{eq}^{cr}, (b) Von Misses stress σ_{eq}, (c) CE22 is hoop creep strain ε_{22}^{cr}.

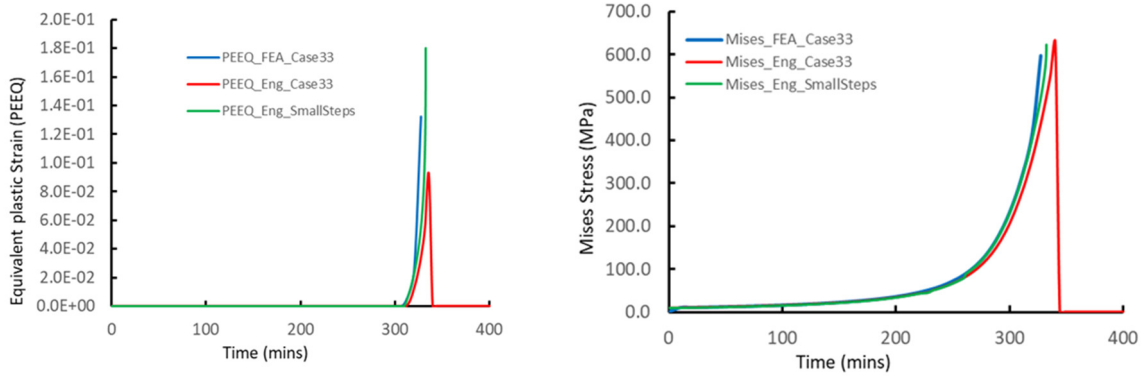

(a) (b)

Figure 11: Comparison of engineering model and FEA results for Case 33: blocked PRV. (a) PEEQ is equivalent plastic strain ε_{eq}^{cr}, (b) Von Misses stress σ_{eq}. Eng_SmallSteps curves show the engineering model results with time increments reduced to 0.1 minutes.

4.1 Capabilities and Limitations

4.1.1 Material

The material model used by CMAT in the FEA and engineering models are valid for TC128B and A516-70 materials from ambient (25 °C) to 800 °C. Some limited testing was completed above 800 °C the material strength becomes so low above 800 °C that no further testing is required. The material strength can be assumed to go to zero. Therefore, the material models are valid for all fire temperatures that a tank car may experience.

The material creep tests were completed that in timeframe that ranged from minutes to many hours. Some extrapolation of the data to a timeframe of several days is reasonable. Extrapolation of this data to weeks or months is not. The material model presented here should not be applied to situations with sustained high temperatures above 400 °C for months or weeks without further testing and validation.

4.1.2 Engineering Model

The engineering model was developed and validated against CMAT's FEA model for standard DOT-117 tank cars in engulfing pool fire scenarios. The model may be suitable for other types of cars, tanks, and fires however it has not been validated for use in these cases.

The inputs to the engineering model are the geometry of the tank, the tank peak wall temperature, and the internal pressure. The accuracy of the engineering model is completely dependent on the accuracy of this input data

The engineering model assumes that the thermal protection is continuous. The model may be suitable for assessing local hot spots if suitable temperature and pressure data were provided however it should be validated against CMAT's FEA model before widespread use in these cases.

5 FIRE SCENARIOS

CMAT was asked to run a series of FE and engineering model simulations using 2D input data provided by CanmetENERGY. CanmetENERGY's heat transfer models had been updated to more accurately represent the heat transferred by radiation to the tank from a fire. This section summarizes the results of those simulations.

5.1 Cases and Input Data

Transport Canada identified several cases for analysis. All cases identified were variations of the base case described in Table 4. For each Case, CanmetENERGY provided CMAT with a dataset that included lading temperature, vapour temperature, and pressure as a function of time up to 716 minutes obtained using Aspen HYSYS process simulation software. The peak tank wall temperature can be assumed to be equivalent to the vapour temperature. Previous computational fluid dynamics (CFD) simulations by CanmetENERGY validated this assumption. This data is required for CMAT's structural tank car simulations using both FEA and the engineering model. An example of this data is shown in Figure 12.

Table 4: Base case (Case 1) conditions for tank car fire simulations

Base Case Conditions (Case 1)	
Fire Temperature	815.6 °C
Fill Level	92.6%
Lading	Light crude oil
Roll angle	0° (Upright)
Shell Thickness	0.5625" (14.2875 mm)
FyreWrap Thickness	0.500"
PRV Discharge Start	75 psig (0.517 MPa)
PRV Full Open	85 psig (0.586 MPa)
PRV Flowrate	30888 SCFM
Fire Emissivity	1
Tank Emissivity	0.9

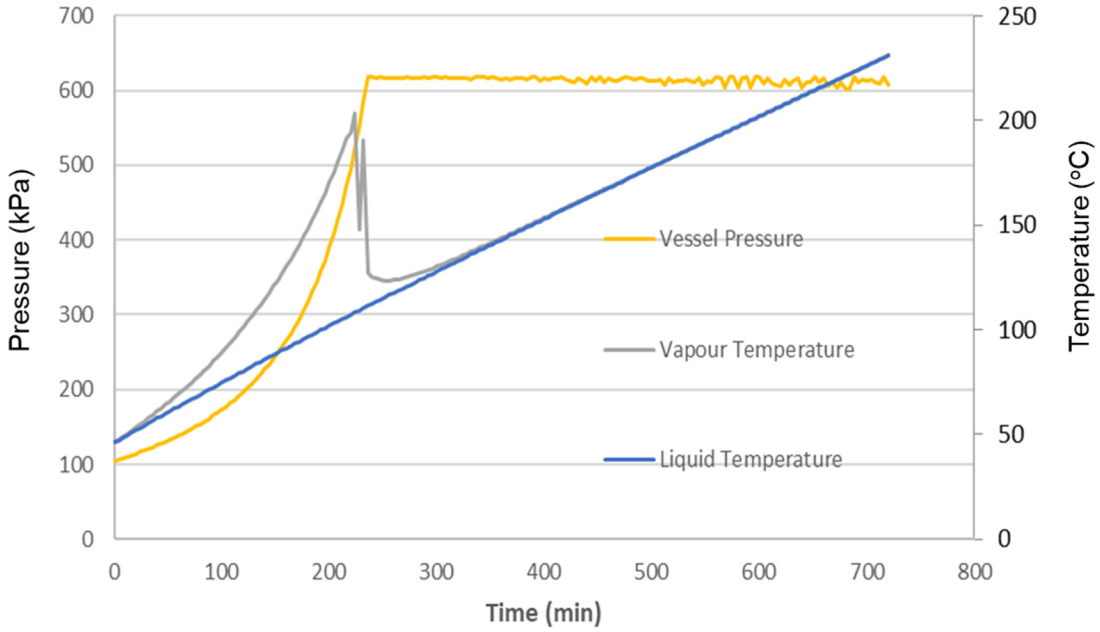

Figure 12: Liquid temperature, vapour temperature, and vessel pressure as a function of time for the base case (Case 1) calculated by CanmetENERGY using HYSYS.

In this data, it can be seen that the vapour temperature increases more quickly than the liquid temperature. When the tank goes to a "shell full" condition around the 210 minute mark due to thermal expansion, the vapour space disappears and the vapour temperature drops to that of the liquid temperature, where they both continue to increase as the run time increases. Meanwhile the pressure increases until it reaches approximately 618 kPa (90 psig).

Since most cases did not fail or have any creep deformation within the 716 minutes of supplied data, CMAT extrapolated the data for some cases to 2400 minutes, with the non-realistic assumption that the pressure remained constant throughout with no release of lading through the PRV. An example of extrapolated data is provided in Figure 13.

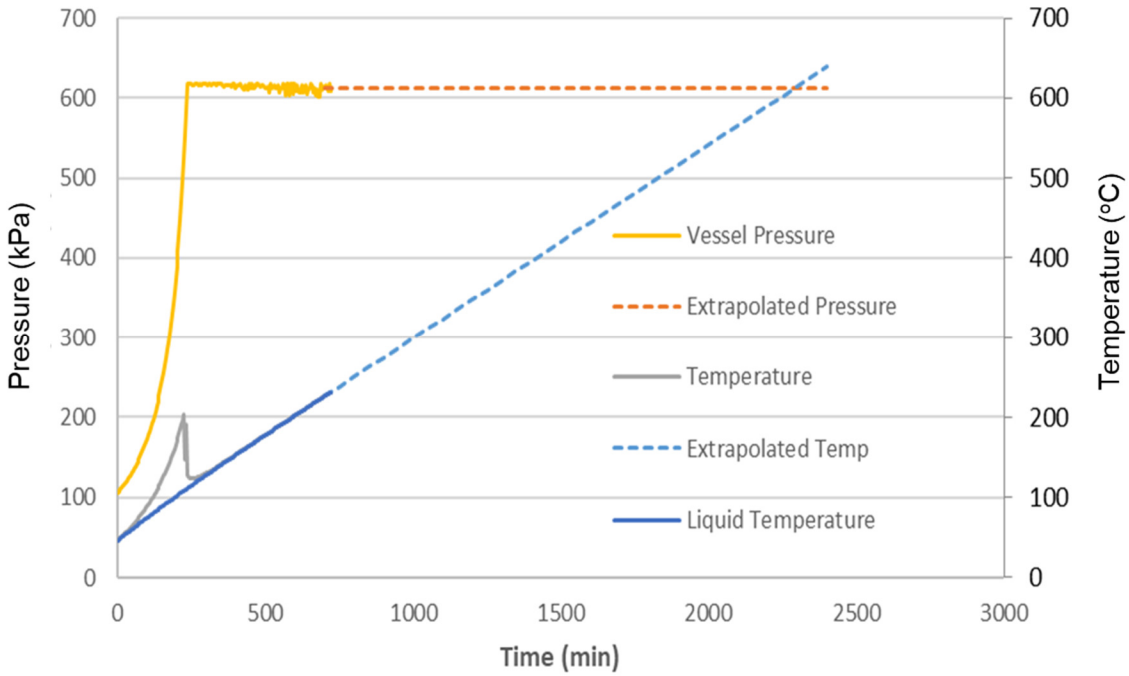

Figure 13: Extrapolated temperature and pressure data (dotted lines) for the base case (Case 1)

6 RESULTS

The results from CMAT's simulations are summarized in Table 5 . Each case was also run in AFFTAC by Transport Canada with technical assistance from Southern Rockies Consulting. A description of each column of Table 5 is as follows:

Case	Number assigned by Transport Canada
Description	Short description of change from the base case
AFFTAC Result	AFFTAC results are listed as pass or burst
AFFTAC Run Time	The time at which the simulation terminated. Cases that ran 716 min. did not burst due to creep.
CMAT Result	CMAT's results are described as: Pass – no creep: No creep, plastic deformation or failure occurred in the 716 minutes of the simulations. Pass – creep: These cases did have creep deformation but it did not result in tank car failure within 716 minutes Burst – plastic: This indicates that the tank car burst due to the hoop stress in the tank car overcoming the strength of the material with little or no creep deformation

	Burst – creep: This indicates that the tank car burst due to accumulated creep deformation. Note that the results for all FEA and engineering simulations were the same.
CMAT Time to failure	A time is listed in this field at the time the tank car ruptured, if it ruptured. Results for FEA and Engineering (ENG) simulations are displayed separately.
Creep Strain at 716 min	For the cases where Creep occurred but the tank car did not burst the total accumulated creep strain at 716 minutes is displayed. Cases that burst have the creep strain at 716 minutes listed as >20.

Table 5: Summary of results from AFFTAC and CMAT's FE and engineering models. CMAT burst results are highlighted in red.

		AFFTAC		CMAT				
					Time to failure		Creep Strain at end of simulation time	
Case	Description	Result	Run Time	CMAT Result	FEA	ENG	FEA	ENG
1	Base case	pass	716	pass – no creep			0	0
2	Base case 45° roll	pass	716	pass – no creep			0	0
3	Base case 120° roll	pass	716	pass – no creep			0	0
4	Fire Temp 850 °C	pass	716	pass – no creep			0	0
5	Fire Temp 900 °C	pass	716	pass – creep			5.0E-07	5.0E-07
6	Fire Temp 950 °C	pass	716	pass – creep			1.0E-06	1.0E-06
7	Fire Temp 1000 °C	pass	716	pass – creep			1.7E-06	1.7E-06
8	Fire Temp 1100 °C	pass	716	pass – creep			3.5E-06	3.4E-06
9	Fire Temp 1204 °C	pass	716	pass – creep			8.1E-06	7.6E-06
10	Fill level 87.5%	pass	716	pass – creep			2.3E-05	2.4E-05
11	Fill level 80%	pass	716	pass – creep			4.3E-04	4.3E-04
12	PRV 165 psig 0° roll	pass	716	pass – no creep			0	0
13	PRV 165 psig 45° roll	pass	716	pass – no creep			0	0
14	PRV 165 psig 120° roll	pass	716	pass – no creep			0	0
15	Shell 0.6188" 0° roll	pass	716	pass – no creep			0	0
16	Shell 0.6188" 45° roll	pass	716	pass – no creep			0	0
17	Shell 0.6188" 120° roll	pass	716	pass – no creep			0	0
18	Shell 0.5063" 0° roll	pass	716	pass – no creep			0	0
19	Shell 0.5063" 45° roll	pass	716	pass – no creep			0	0
20	Shell 0.5063" 120° roll	pass	716	pass – no creep			0	0
25	Crude type heavy	pass	716	pass – creep			1.6E-05	1.6E-05
26	Crude type condensate	pass	716	pass – no creep			0	0
27	Tank emissivity 0.92	pass	716	pass – no creep			0	0
28	Tank emissivity 0.8	pass	716	pass – no creep			0	0
29	Tank emissivity 1.0	pass	716	pass – no creep			0	0
30	Crude type dilbit	pass	716	pass – creep			2.4E-05	2.4E-05
31	Restricted PRV (50%)	pass	716	pass – no creep			0	0
32	Restricted PRV (80%)	pass	716	pass – no creep			0	0
33	Blocked PRV (100%)	pass	716	burst – plastic	327.5	340*	0	0
34	Bare shell	pass	716	burst – creep	675	676	> 20	> 20

* When run with 0.1 minute time increments the time of failure was 332.4 minutes.

All cases run in AFFTAC, CMAT's FEA model, and CMAT's engineering model passed the test requirements of TP14877 by surviving at least 100 minutes. Note that Case 9 survived with a fire temperature of 1204 °C, equivalent to the torch fire temperature of TP14877. It is therefore reasonable to assume a localized hot spot (torch) at this temperature would also be survived.

Due to the number of cases that did not experience creep or failure a select few cases were extrapolated to 2400 minutes in the CMAT FEA and engineering models. The results of these cases are shown in Table 6. The results of these cases must be appreciated with caution because the temperature and pressure results were not modeled rigorously. For each case the pressure was assumed to remain constant and the temperature was assumed to increase linearly over time, with no corresponding release of tank lading. These results do not indicate or stop when the tank would have emptied. The extrapolated cases were created to test and compare the engineering and FEA models and should not be considered a prediction of realistic scenarios.

Table 6: Results from selected extrapolated CMAT cases. Burst results are highlighted in red.

CMAT Extrapolated Results							
			Failure Time			Creep Strain at end of simulation time	
Case	Description	CMAT Result	FEA	Eng.	% Difference	FEA	Eng.
1	Base case	pass - creep				0.013602	0.017336
2	Base case 45° roll	burst - creep	1350	1300	3.7%	> 20	> 20
3	Base case 120° roll	pass - creep				0.023312	0.029366
9	Fire Temp 1204 °C	burst - creep	1550	1500	3.2%	> 20	> 20
12	PRV 165 psig 0° roll	burst - creep	2080	2050	1.4%	> 20	> 20
13	PRV 165 psig 45° roll	burst - creep	1210	1200	0.8%	> 20	> 20
14	PRV 165 psig 120° roll	burst - creep	2300	2300	0.0%	> 20	> 20

7 DISCUSSIONS AND COMPARISONS

7.1 General Results

The results demonstrate that the modelled TPS, which includes a 0.5” ceramic blanket (also known as FyreWrap) is effective in preventing creep deformation when exposed to high temperatures. The CanmetENERGY and CMAT results predict that the only case with the TPS that would fail in less than 716 minutes is Case 33 with the fully blocked PRV, and no cases fail before 100 minutes. AFFTAC predicted that all cases would pass, both at 100 and 716 minutes.

7.2 Extrapolated Results

Cases 1, 2, and 3 differ only by their roll angles of 0°, 45°, and 120° respectively. Only extrapolated Case 2 was predicted to fail under 2400 minutes. The internal pressure in all cases was the same (618.2 kPa or 90 psig), slightly higher than the full open pressure (85 psig) of the modeled PRV. The predicted temperature for Case 2 was much higher than Cases 1 and 3 (Figure 14). The reason for this is not known at this time, and further cases would need to be run to investigate further. In Case 3, the overturned tank car would be releasing liquid through the PRV for the entire relief period, and while liquid flow is more efficient at emptying mass from a tank, it is not as efficient at reducing the pressure in a tank. This trend would also be seen for Case 2, to a lesser extent, as the lower degree of rollover would mean that liquid will discharge until the lading level is below

the PRV, after which the PRV will discharge vapour. HYSYS boundary condition inputs may need to be revisited to explain this trend. However, this is outside the scope of this work.

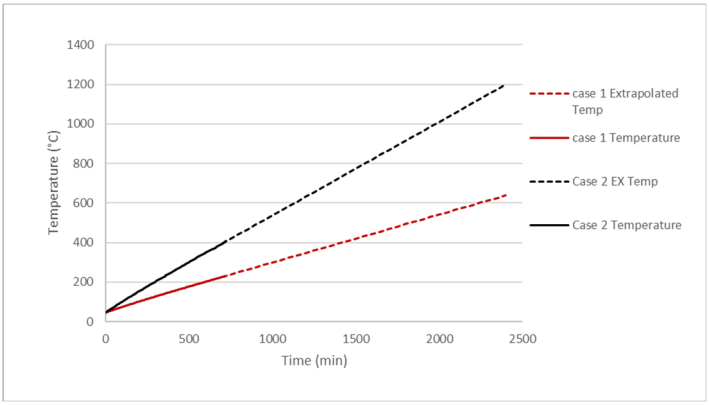

Figure 14: Extrapolated liquid temperature for Cases 1 and 2. Case 3 temperature was very close to Case 1.

Case 9 differs from Case 1 only by a higher fire temperature of 1204°C. Predictably, the increased temperature resulted in higher creep in Case 9 and failure after 1550 minutes, rather than survival to 2400 minutes for Case 1.

Cases 12, 13, and 14 were repeats of Cases 1, 2, and 3 with higher PRV release pressures, and as a result had the same heating trend of Cases 13 and 2 being higher than the others, as discussed previously. Each higher PRV set pressure case resulted in failure before 2400 minutes, with higher creep rates at the failure time compared to the same time in Cases 1, 2, and 3.

7.3 CMAT FEA to Engineering Model Comparison

The FEA and engineering models produced the same result (pass-creep, pass-no creep, or burst) for all cases studied including the extrapolated cases. The difference in predicted time to failure between the two models was less than 5% for all cases studied so far. Due to the limited number of cases which resulted in creep and failure there is limited data available for comparing the two models. Running cases at higher temperatures and pressures would better test the models even though they are less realistic. The case with the largest difference was Case 33 with the blocked PRV valve. FEA predicted a failure time of 327.5 minutes and the engineering model predicted 340 minutes. This was the only plasticity-dominated case. When a smaller time increment (0.1 minute) was used in the engineering calculations the predicted time to failure reduced to 332.4 minutes. This was the only case that was found to be time increment dependent. It is recommended that any case that has significant plasticity should be re-run using a smaller time increment or should be analysed with FEA.

The engineering model can be run in any standard spreadsheet (MS Excel in this case) and could easily be implemented as a simple program. Results are obtained as soon as the input data is provided. The FEA model requires the use of commercial software (Abaqus FEA) and can take between tens of minutes and hours to run a case depending on the conditions. An important distinction is that FEA models can capture complex stress states, whereas the engineering model only considers the stress state in the head or wall.

7.4 Canmet Energy Scenarios

The updates completed this year to CanmetENERGY's thermal model had a significant impact on the temperature. In a previous report over 30 independent cases were presented (*Finite Element Simulation of Rail Tank Car Creep Failure in an Engulfing Fire Scenario*, Jonathan McKinley, 2020). All cases exhibited significant amounts of creep deformation, and most failed within 100 to 600 minutes. In the results of simulations performed for this report, only two cases failed within the 716 minute timeframe. Case 33 burst plastically due to a completely blocked PRV valve and Case 34 (bare shell case without thermal protection) failed due to accumulated creep. The reason for this change is much lower peak shell temperatures. Figure 15 shows the temperature and pressure supplied by CanmetENERGY for Case 1 and Case 34. Both cases show a sudden drop in the peak temperature as the lading inside the tank expands and the vapour space disappears in the shell full condition. Although this would result in venting liquid it does have a protective effect of lowering the peak wall temperature. This, combined with the thermal protection system, prevents creep from occurring in the base case. Case 34 does see the peak temperature rise again later in the simulation, ultimately resulting in failure at 675 minutes (FEA).

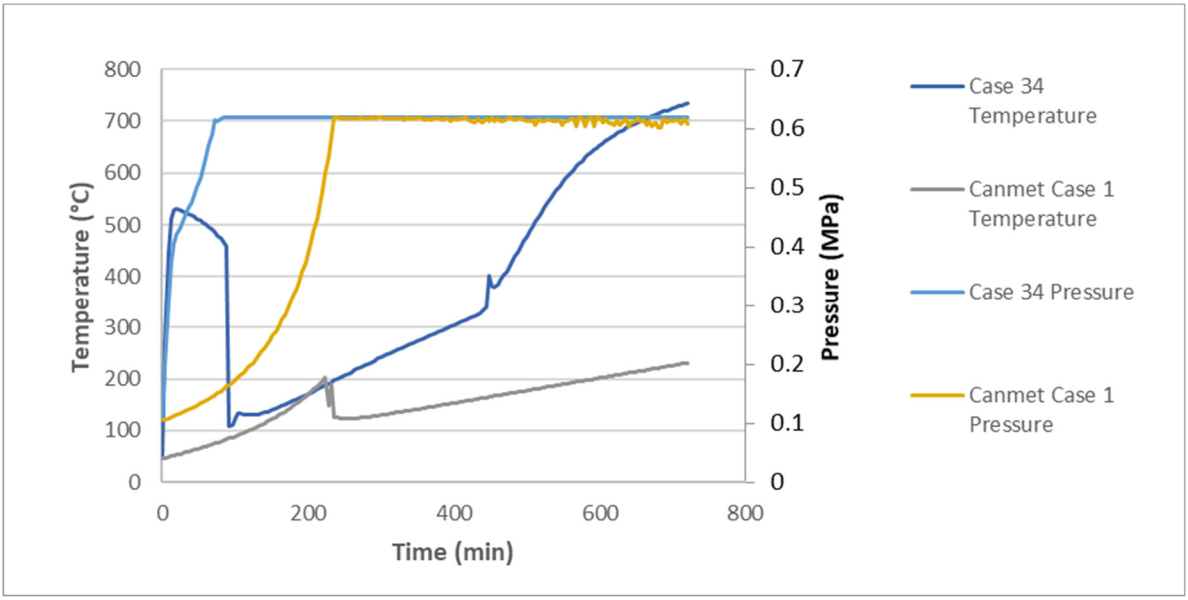

Figure 15: Vapour (peak) temperature and pressure supplied by CanmetENERGY for Case 1 (base case) and Case 34 (bare shell).

7.5 CanmetENERGY and AFFTAC

The vapour temperature and pressure data from AFFTAC and CanmetENERGY are quite different in many cases, an example of which is shown in Figure 16 (Case 1). AFFTAC maintains the tank pressure at the start-to-open pressure setting of 75 psig (0.52 MPa), while the CanmetENERGY data shows the tank pressure as increasing to just over 89 psig (0.62 MPa), rather than the full open pressure of 85 psig (0.58 MPa). Regarding temperature, AFFTAC predicts that the rate of vapour space temperature increase decreases over time, reaching a maximum of 210 °C during the 716 minute run. The CanmetENERGY data shows an increase to 203 °C, followed by a drop in vapour

temperature when the tank goes shell-full at 224 minutes, and then a subsequent steady increase throughout the rest of the run. These discrepancies in the pressure and temperature inputs will have an effect on the outcomes of the material models, and should be investigated and rectified before conclusions regarding comparisons of the model outcomes are finalized.

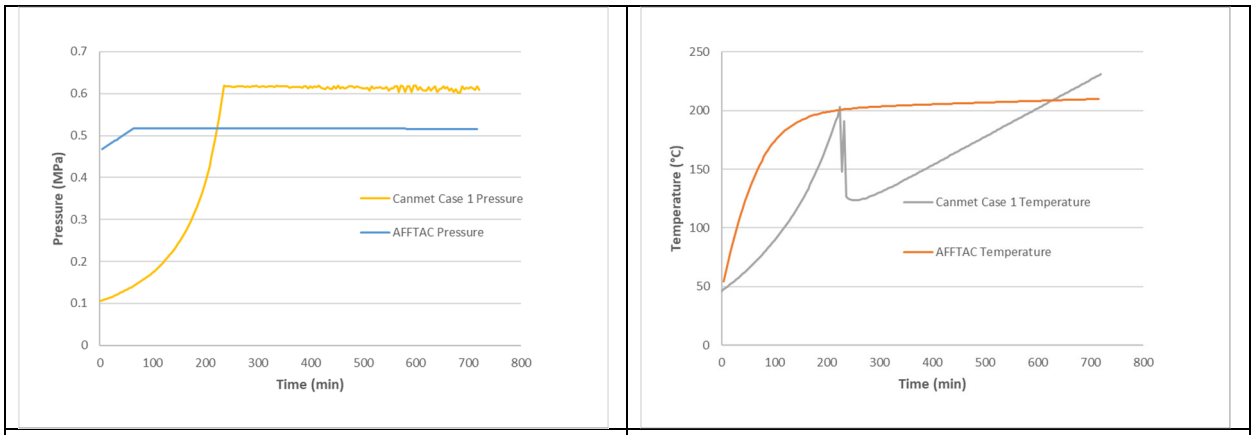

Figure 16: Comparison of AFFTAC and CanmetENERGY pressure (a) and vapour space temperature (b) curves for Case 1.

AFFTAC results for Case 1 (lading temperature, max wall temperature, interior and burst pressure, and fraction filled) are shown in Figure 17 for comparison with selected cases throughout this section.

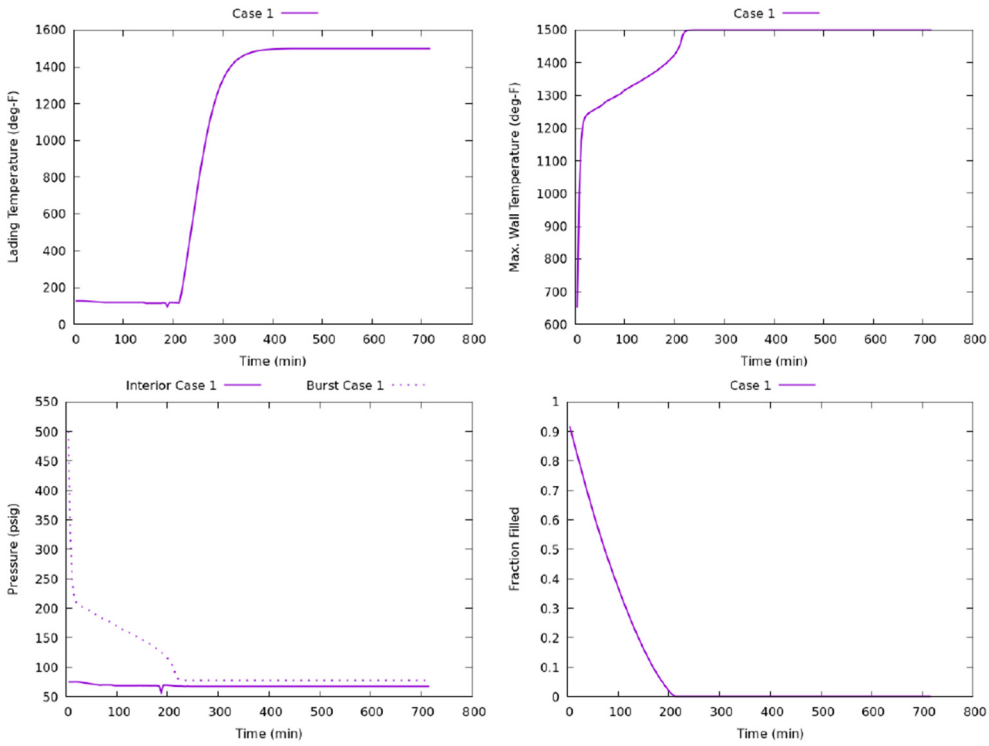

Figure 17: AFFTAC results (temperature, pressure, and fraction filled) for Case 1.

7.6 AFFTAC to AFFTAC

Cases 1b, 2b, and 3b had the exact same boundary conditions as Cases 1, 2, and 3. Cases 1, 2, and 3 were run with a tank steel input to the AFFTAC StrengthModel.db database by TC using NRCan CMAT-supplied TC 128B steel test data. The data was supplied for two strength models: ultimate tensile strength (UTS) and Larson-Miller. AFFTAC runs the two strength models at the same time, and failure is declared when either indicates failure.The UTS test data was available for low temperatures only, and so AFFTAC would have to extrapolate linearly to the fire temperatures, which can introduce uncertainty. Cases 1b, 2b, and 3b were run using the "AAR TC128-70, Grs. A & B Min. Tensile strength 81 Kpsi" steel available in the version of StrengthModel.db supplied in the AFFTAC download. This steel has a default nominal burst pressure of 850 psig, and all emissivity values were set to be equivalent to the base case steel. These cases are compared in Table 7. As presented above, all of the base case, TC-input material cases ran for the full 716 minutes without failure. None of the AFFTAC-database material cases survived. Case 3b failed in the shortest period of time, 60 minutes. The peak temperature and pressure inside the tank car are also listed in Table 7. All cases had a peak pressure of 0.52 MPa (75 psig). The peak temperatures were all below 300 °C. Case 3 reached the highest temperature of 291.2 °C. CMAT's material model does not predict any creep at these temperatures. At 291.2 °C and 0.52 MPa pressure CMAT's engineering model predicts that the Von Mises stress in the tank wall would be 42 MPa and the yield stress would be 334 MPa resulting in a safety factor of almost 8. It appears that the AFFTAC-database TC 128B steel is more conservative. This may be due to the extrapolation of the TC-input steel data to the fire temperatures. No further conclusions can be drawn without reviewing the material data itself.

Table 7: Comparison of Cases 1, 2, and 3 run in AFFTAC using standard material and alternate material. Peak AFFTAC temperature, pressure, and CMAT results are shown as well.

		TC-Input Material (base cases)		AFFTAC-database Material (b-Cases)		Peak Temperature	Peak Pressure	CMAT Result
Case	Description	Result	Run Time	Result	Run Time	°C	MPa	
1	Base case	pass	716	burst	184	209.9	0.52	pass - no creep
2	Base case 45° roll	pass	716	burst	180	210.9	0.52	pass - no creep
3	Base case 120° roll	pass	716	burst	60	291.2	0.52	pass - no creep

8 ALTERNATIVE CASES

Although the effectiveness of the thermal protection system (TPS) at preventing creep deformation is a desirable result in accident scenarios, the slow ramp in temperature in the studied simulations means that the models were not tested under more severe conditions that could be expected to cause higher creep. Additionally, because the boundary conditions provided by CanmetENERGY and those calculated by AFFTAC in the above cases did not match, it did not provide an effective means of directly comparing CMAT's model to AFFTAC. To address these issues, a number of AFFTAC cases were run with non-standard, less protective TPS, which allows an assessment of tank car model performance in more severe thermal environments. These cases do not reflect TPS requirements as defined by tank car standards. The results are presented here only to make comparisons between the mechanical component of AFFTAC and this work's engineering model in terms of material stress and tank outcomes.

AFFTAC includes a thermal model and a mechanical model in one package. AFFTAC's method of failure prediction is similar to CMAT's in that it can predict yielding using temperature dependent data and it can predict failure due to creep deformation. All cases listed above in Table 5 were run again with greatly reduced thermal protection, leading to rapid increases in steel temperatures and early release of material through the PRV. The temperature and pressure from AFFTAC was used as an input into CMAT's engineering model. Since AFFTAC and CMAT models are using the same temperature and pressure conditions this is an effective method of comparing the models.

Note that AFFTAC is capable of predicting creep as a function of time however the data that CMAT received did not report any creep strain, even in cases that burst, because no failure creep strain data was included in the AFFTAC Strength.db database for the simulated steel, as required when running version 4.00 of AFFTAC. In the presented cases, the AFFTAC strength model is being driven by temperature, as opposed to stress, because the pressures are relatively low and constant in comparison to temperatures.

Fire Temperature

The results from modified Cases 1, 4, 6, and 7 are shown in Table 8Table 8, and in Figure 18. The only difference between each of these cases is the fire temperature. The two lower temperature cases show that CMAT predicts failure in less time than AFFTAC itself. This demonstrates that CMAT is predicting a higher rate of creep for the given conditions. CMAT did not predict failure before AFFTAC in the higher temperature cases (6 and 7); once rupture occurs AFFTAC stops calculating temperature and pressure, and so boundary data is not available to continue the CMAT simulation. At the time the data stopped for Case 6, CMAT had predicted 17.9% strain indicating that failure would occur soon if the simulation continued. Only a reduction in temperature would have prevented failure in Case 6. For Case 7 CMAT had only predicted 2.3% strain by the time AFFTAC predicted failure. As with Case 6, Case 7 would have resulted in failure eventually if the temperature and pressure remained constant or increase. It is difficult to be certain of the reason for the different results without creep output from AFFTAC, however a hypothesis can be made. All AFFTAC cases failed when the steel temperature exceeded 800 °C, and the burst pressure plot has a trajectory similar in shape but opposite in direction to the maximum tank wall temperature plot, indicating that temperature is the driver of failure in these cases. The failures occur when the

interior pressure is low, and would lead of a fairly non-energetic release of liquid. At 800 °C in CMAT's engineering model the yield stress of TC128B is about 50 MPa. The hoop stress in the tank car is also approximately 50 MPa in these cases. CMAT's engineering model calculates yielding; however, it does not predict that the tank will immediately burst. AFFTAC likely stops the simulation as soon as burst stress exceeds interior pressure. CMAT's two models appear to be more conservative on creep prediction and less conservative on yield prediction than AFFTAC.

Table 8: Select results of modified cases with reduced TPS run in AFFTAC and CMAT's engineering model with the same temperature and pressure boundary conditions.

	Fire Temp. (°C)	**AFFTAC Failure Time (minutes)**	**AFFTAC Failure Temp. (°C)**	**CMAT Failure Time (minutes)**	**CMAT Failure Temp. (°C)**	**Notes**
Case 1	815.6	No Failure	815.6	152	741.6	
Case 4	850	184	815.6	100	752.8	
Case 6	950	60	821.5	*	N/A	*CMAT Creep of 17.9% at 60 minutes. Failure would have occurred soon.
Case 7	1000	12	811.8	**	N/A	**CMAT Creep of 2.3% at 12 min. Would fail eventually

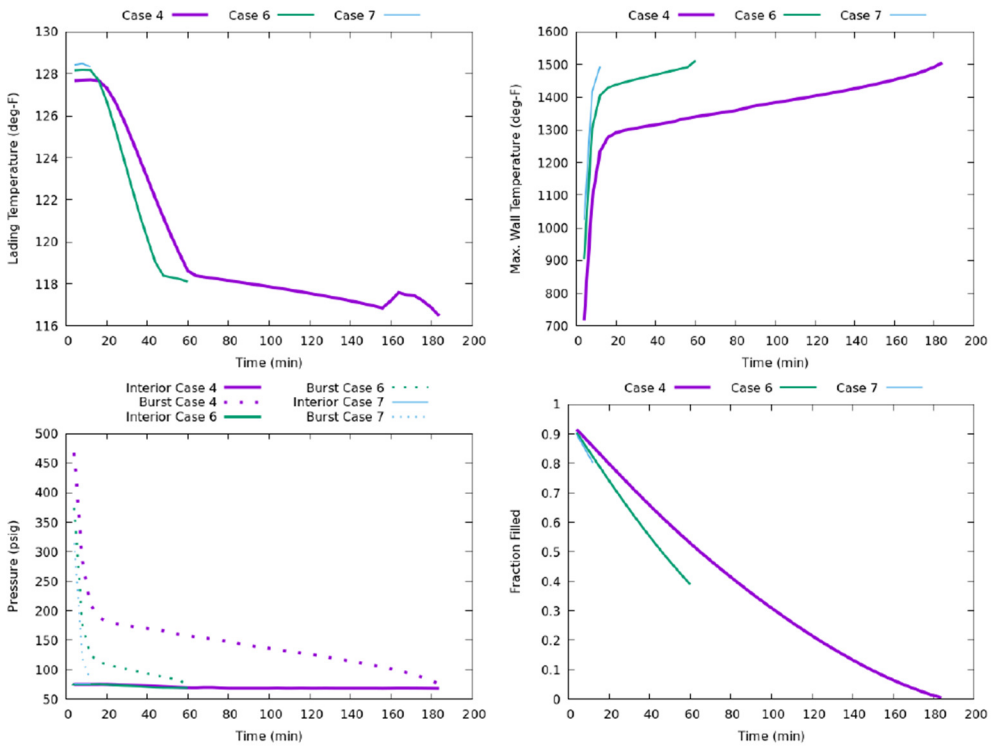

Figure 18: AFFTAC results (temperature, pressure, and fraction filled) for Cases 4, 6, and 7.

PRV Release Pressure

Cases 12, 13, and 14, were repeats of Cases 1, 2, and 3 with a higher PRV release point of 165 psig. AFFTAC predicted that the modified Cases 1, 2, and 3 would not fail, while CMAT predicted that they would. AFFTAC and CMAT both predicted that Cases 12, 13, and 14 would burst. CMAT predicted much shorter times until rupture as shown in Table 9. One contributor to this difference is how CMAT calculates stress. Figure 19 shows AFFTAC and CMAT's stress calculations along with pressure. AFFTAC predicts that the stress follows the pressure. CMAT predicts that the stress continues to increase due to wall thinning.

Note that the temperature at the time of failure in the AFFTAC cases was lower in Cases 12, 13, and 14; between 715 and 730 °C (1319 and 1346 °F; Figure 20). Once again CMAT's model would predict yielding at that point.

Table 9: Cases with high PRV release point (165 psig) modified with reduced TPS. AFFTAC and CMAT's engineering model used the same temperature and pressure boundary conditions. Data from Case 1 (75 psig release pressure) included for reference.

	AFFTAC Failure Time (minutes)	**AFFTAC Failure Temp. (°C)**	**AFFTAC Peak Stress (MPa)**	**CMAT Failure Time (minutes)**	**CMAT Failure Temp. (°C)**	**CMAT Peak Stress (MPa)**
Case 1	N/A	N/A	47.8	153	739.4	51.1
Case 12	144	733.2	104.8	40	673	119.6
Case 13	132	731	97.6	36	677	108.6
Case 14	28	713.8	111.2	20	662	113.9

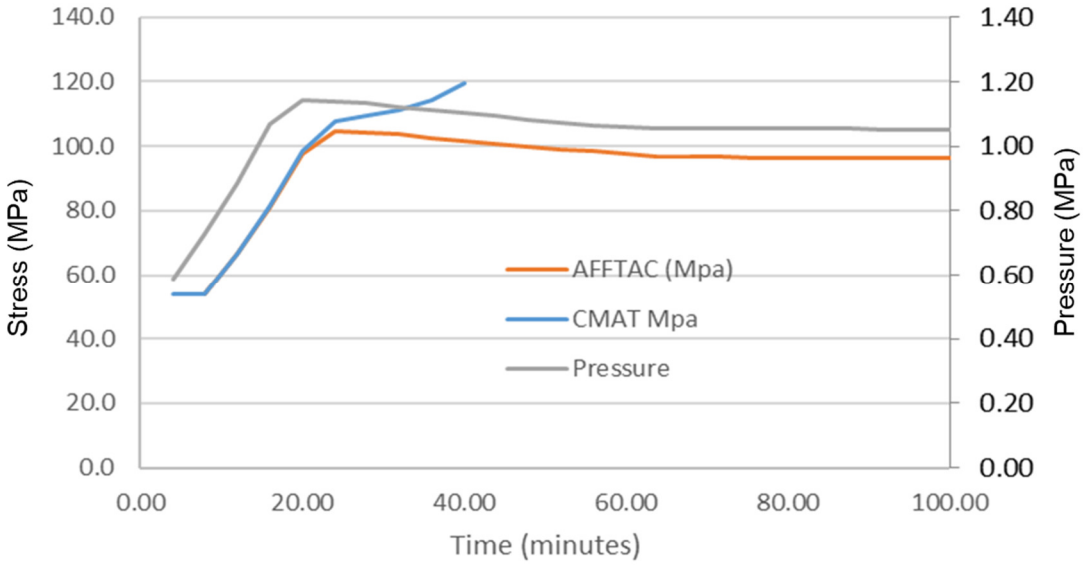

Figure 19: Pressure and stress predictions from AFFTAC and CMAT engineering model for modified Case 12 with reduced TPS.

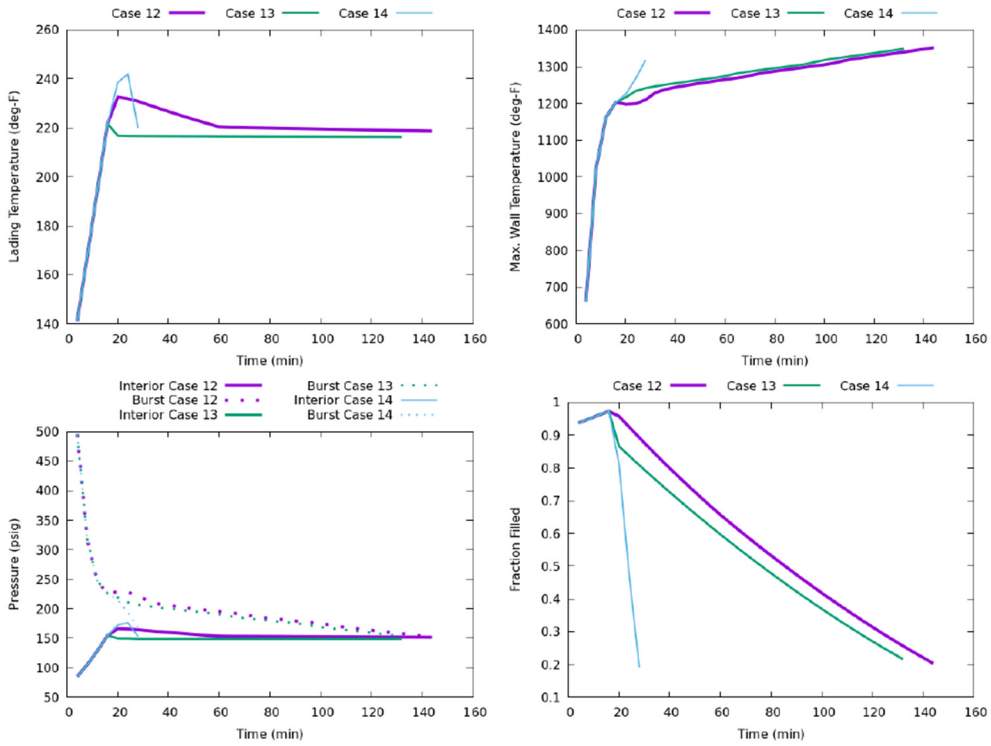

Figure 20: AFFTAC results (temperature, pressure, and fraction filled) for Cases 12, 13, and 14.

Shell Thickness

Cases 15 to 20 are repeats of Cases 1, 2, and 3 with different shell wall thicknesses. AFFTAC predicted no failure for Cases 15 to 20. Cases 1, 15, and 18 were identical except for the wall thickness. Case 15 had the wall thickness increased 10% while Case 18 had a 10% reduction. The reduced wall thickness resulted in a 36 minute or 23% reduction in the time to failure as shown in Table 10.

Table 10: Results of Cases 1, 15, and 18 run on CMAT's engineering model using AFFTAC's temperature and pressure boundary conditions.

	Wall thickness (in)	**CMAT Time to Failure (min)**	**AFFTAC Time to Failure (min)**
Case 1	0.5625	156	N/A
Case 15	0.6188	184	N/A
Case 18	0.5063	120	N/A

Restricted PRV

Cases 31, 32, and 33 are repeats of Case 1 with PRV restriction of 50%, 80%, and 100% respectively. The case with 50% restriction resulted in no change in the internal pressure. 80% restriction resulted in an initial pressure spike that dissipated as shown in Figure 21. Case 33 with 100% restriction resulted in significantly higher pressure. AFFTAC did not predict failure in either Case 31 or 32 while CMAT did predict failure. In these two cases the AFFTAC-estimated interior

pressure is very low, yet it is very close to the burst pressure for a significant length of time without bursting (Figure 22) due to the sustained high temperatures. This behaviour would warrant further closer analysis if more information was needed about these cases, to understand the effect of small changes in inputs on the failure times. AFFTAC predicted failure of Case 33 in 24 minutes. CMAT's engineering model did not predict failure under 24 minutes. At 24 minutes the CMAT model predicted a stress (σ_{eq}) of 135 MPa, which is above the 113 MPa yield (σ_y)) but below the 178 MPa UTS (σ_u)) at 652 °C. At 24 minutes, 6% Creep strain had occurred. If the data continued it is expected that CMAT's model would predict failure soon after 24 minutes.

Table 11: Results of Cases 1, 31, 32, and 33 showing the effect of restricted PRV valve. Run on CMAT's engineering model using AFFTAC's more severe temperature and pressure boundary conditions.

	PRV Restriction	**AFFTAC Failure Time (min)**	**AFFTAC Failure Temp. (°C)**	**CMAT Failure Time (min)**	**CMAT Failure Temp. (°C)**
Case 1	0 %	N/A	N/A	156	741.8
Case 31	50 %	N/A	N/A	156	741.8
Case 32	80%	N/A	N/A	52	681.7
Case 33	100%	24	652.5	*	*

* CMAT's model did not predict failure with the available data up to 24 minutes, but would have predicted failure shortly after if data had continued.

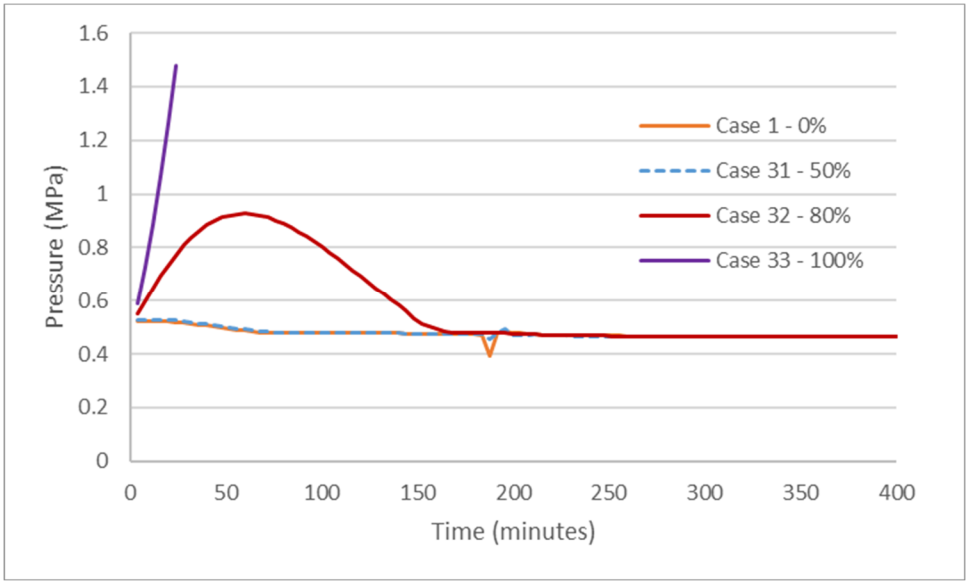

Figure 21: Pressure profiles from Cases 1, 31, 32, and 33 showing progressive levels of PRV blockage 0%, 50%, 80%, 100%.

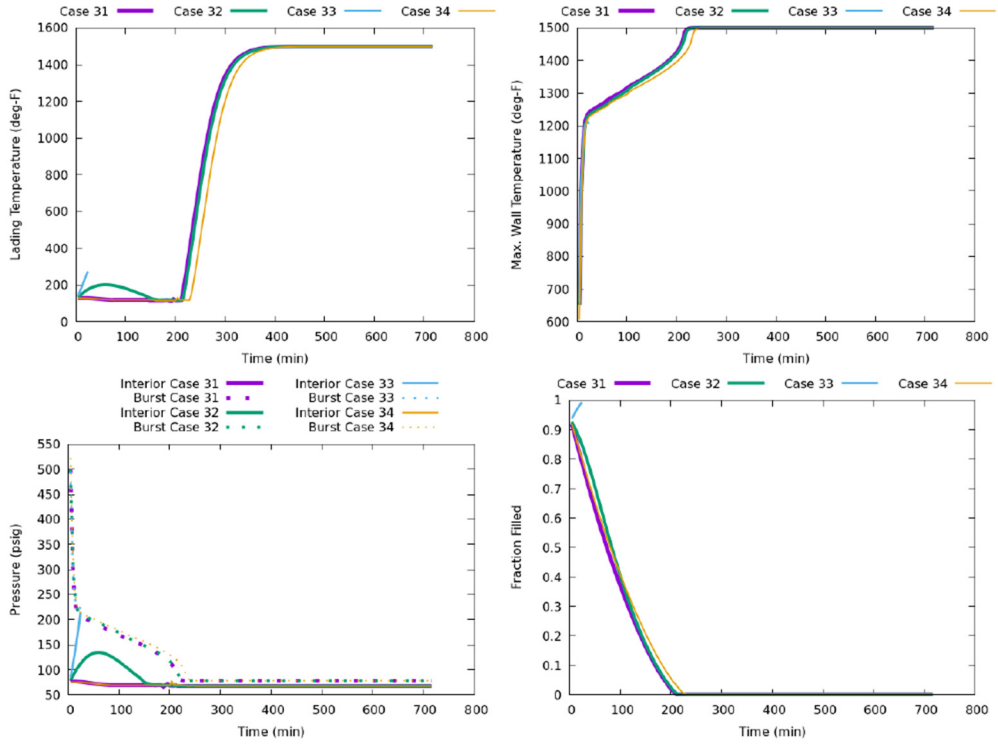

Figure 22: AFFTAC results (temperature, pressure, and fraction filled) for Cases 31, 32, 33, and 34.

Bare Shell

Case 34 is the bare shell scenario. AFFTAC predicts that this case will pass, but the interior pressure is very low (Figure 22), yet it is very close to the burst pressure for a significant length of time without bursting due to the high temperature. This raises the concern that a small change in input temperature or pressure might result in a low energy release of liquid from a nearly-empty tank. The AFFTAC data provided shows a wall temperature of 815 °C that is maintained for several hundred minutes. Both AFFTAC and CMAT models would typically predict a failure after sustained time above 800 °C. This is the only case that the CMAT model predicts a creep failure. The FEA and engineering model predictions are within a minute of each other which shows that the simplifications made are satisfactory.

Table 12: Results of bare shell case with no thermal protection. Run on CMAT's engineering model using AFFTAC's more severe temperature and pressure boundary conditions.

	AFFTAC Failure Time (min)	**AFFTAC Failure Temp. (°C)**	**CMAT Failure Time (min)**	**CMAT Failure Temp. (°C)**
Case 34	N/A	N/A	156	741.8

9 CONCLUSIONS

An engineering model for calculating creep and plastic deformation in tank cars in fire scenarios was developed based on the typical stress state in the tank car. Thirty four simulated fire scenarios were analysed by CanmetENERGY to produce temperature and pressure boundary conditions for CMAT's FEA and engineering models. The models demonstrated the effectiveness of the thermal protection system of DOT-117 tank cars since only the bare shell and blocked PRV cases resulted in failure, both well past 100 minutes of run time. The scenarios were also run on the program AFFTAC and did not predict failure in any of the cases. The engineering model produced very similar results to CMAT's FEA model.

One objective of this work was to compare the results of AFFTAC to CMAT's two models. This was difficult to achieve as there were few results producing failure and since AFFTAC includes both a thermal model and a mechanical model in one package, compared to CMAT's mechanical model. Consequently, alternative scenarios with less protective non-standard TPS were run in AFFTAC. AFFTAC's temperature and pressure data was used as an input to CMAT's engineering model allowing a direct comparison between the two. The results showed that CMAT's model tends to predict a higher rate of creep than AFFTAC. AFFTAC appears to predict failure once yielding (plastic deformation) occurs. CMAT calculates the yield deformation and allows the prediction to continue until the UTS is passed. Neither model is consistently more or less conservative than the other. For plastic deformation conditions, CMAT's models tend to be more conservative than AFFTAC's creep and UTS models.

9.1 Overview of CMAT to AFFTAC Material Models

The comparison between CMAT and AFFTAC models discussed throughout this report are summarized in this section. Note that CMAT's material model is used in both the engineering model and the FEA simulations.

9.1.1 Similarities

Both models describe the high temperature behaviour of tank car materials. They both can predict two failure modes; yield (plasticity) and creep. Both models are temperature dependent. As the temperature increases the yield stress decreases. At higher temperatures creep deformation occurs more rapidly at a given stress level than at lower temperatures.

9.1.2 Differences

CMAT uses the hyperbolic sine model to describe creep while AFFTAC uses Larson-Miller. A detailed description of the differences between these models is beyond the scope of this report. In general, Larson-Miller analysis was developed in the 1950s to allow engineers to predict creep behaviour using relatively simple calculations using limited data. Larson Miller analysis lends itself to hand calculations since it does not require updated stress due to material thinning, has few parameters, and can be calibrated with relatively small data sets. The hyperbolic sine model is better suited for use with FEA. The hyperbolic sine model can be more difficult to fit to experimental data and to calculate outcomes due to the large number of parameters. Both models

interpolate between and extrapolate from experimental data. CMAT conducted extensive testing of tank car materials TC128B and A516-70 under the range of temperatures and stresses that would be seen in a fire scenario to prevent extrapolation. Over 25 independent conditions were tested for each material. The AFFTAC data set, input by TC based on NRCan test data, is much smaller and over a lower temperature range, which means that extrapolation is more likely.

Both CMAT and AFFTAC use temperature dependent yielding. During a simulation, AFFTAC stops simulations when failure occurs, based on temperature-dependant UTS or creep. CMAT calculates the deformation that occurs after yielding and allows simulations, engineering or FEA, to continue.

9.1.3 Assumptions

The assumptions of CMAT's engineering model stated above are that failure occurs at the point of peak temperature and failure occurs due to localized accumulated strain. AFFTAC keeps a record of the creep at 180 points around half of the circular cross section, and creep history accumulates differently at each point based on temperature change. Failure occurs when any one of the points fails, not necessarily at the location of peak temperature. The FEA model does not assume that failure occurs at the point of peak temperature. All FEA results so far support this assumption.

CMAT also assumes that creep deformation follows plasticity theory. This assumption is relevant to the hyperbolic sine model but not to Larson-Miller.

The peak tank wall temperature is assumed to be equivalent to the vapour temperature though this assumption is for the input data supplied to CMAT not the material model. AFFTAC allows the wall temperature over the vapour to be different than the vapour temperature, but the vapour temperature is assumed to be the same as the liquid temperature.

CMAT's engineering model and AFFTAC both assume that the tank car acts as a thin-walled pressure vessel meaning that the stress and strain are the same at the inside and the outside of the tank shell. This is a standard assumption. The FEA model does allow for through thickness stress, strain, and temperature. The influence was not significant.

9.1.4 Methodology

The differences in methodology are covered in the section on similarities and differences above. Both models use similar approaches with the main difference being that CMAT chose to use more complex models to describe plasticity and creep. The most significant difference between the models may be the amount of experimental data. Because this data can be user-supplied, as in the case of this project, it can greatly impact the results of any AFFTAC analysis.

10 FUTURE WORK

Some potential future work to consider includes:

As stated above a significant difference between CMAT and AFFTAC is the amount of experimental data that the models rely on. CMAT's data can be added to AFFTAC's databases. CMAT's yield data for TC128B and A516-70 can likely be added very easily. CMAT's creep data could be analysed to calculate Larson-Miller parameters to include in AFFTAC as well. Implementing plasticity calculations and the hyperbolic sine model in AFFTAC would be more complex but likely still feasible.

It may also be useful to directly compare the material data used in AFFTAC to that used in CMAT's simulations. This may yield more clear results than comparing the results of the simulations.

It has become clear that local temperatures are the most significant driver of tank car failure in a fire scenario. The work to date assumes that the fire protection is uniform, complete, and undamaged. A failure or gap in the thermal protection could adversely affect fire performance. Similarly most tank cars in fire scenarios have been in an accident and may have sustained damage. Analysis of a damaged tank car can be conducted.

CMAT's engineering and FEA models are compared in this work. The cases used were chosen to represent a variety of different variables. The main temperature used was chosen as it is the temperature required under the applicable standards in TP 14877, however, as a result, many of the cases did not result in failure or creep which reduced the amount of data available for comparison. If additional quantified comparison data is desired additional cases would be run using input data from CanmetENERGY or AFFTAC with more severe conditions (e.g. elevated fire temperatures, reduced thermal protection, or reduction in pressure relief capacity).

11 ACKNOWLEDGEMENTS

The authors would like to thank Transport Canada's Transportation of Dangerous Goods Directorate for funding this work. They would also like to acknowledge the contributions of Michael Spiess, Rachel Domaratzki, and Ian Whittal at Transport Canada. The authors would also like to thank Dr. Scott R. Runnels of Southern Rockies Consulting, LLC for providing AFFTAC support and reviewing this report.

12 REFERENCES

Baličević P, K. D. (2008). *Strength of pressure vessels with ellipsoidal heads.* J Mech Eng 2008;54:685–92.

Jonathan Mckinley, B. W. (2020). *Finite Element Simulation of Rail Tank Car Creep Failure in an Engulfing Fire Scenario.* Canmet Materials, Natural Resources Canada.

Mckinley, J., & Simha, H. (2018). *High-Temperature Mechanical Properties of ASTM 516 Grade 70 Plate - Testing and Analysis.* Natural Resources Canada, CanmetMATERIALS.

Mckinley, J., Xu, S., & Gesing, M. (2018). *Strength, Creep, and Toughness of Two Tank Car Steels - TC128B and A516-70.* Natural Resources Canada, CanmetMATERIALS.

Simha, H. (2016). *Mechanical Properties of Tank Car Steels at Flame Temperature and Modeling of Failure - A Review.* Natural Resources Canada, CanmetMATERIALS.

Simha, H., & Mckinley, J. (2017). *High-Temperature Mechanical Properties of Tank Car Steel - Testing and Analysis.* Natural Resources Canada, CanmetMATERIALS.

W.F. Chen, D. H. (1988). *Plasticity for Structural Engineers.* Springer.